Quantitative Economics 8 (2017), 611–650 1759-7331/20170611

Solving the Diamond–Mortensen–Pissarides model accurately

Nicolas Petrosky-Nadeau
Economic Research, Federal Reserve Bank of San Francisco

Lu Zhang
Fisher College of Business, The Ohio State University and NBER

An accurate global projection algorithm is critical for quantifying the basic moments of the Diamond–Mortensen–Pissarides model. Log linearization understates the mean and volatility of unemployment, but overstates the volatility of labor market tightness and the magnitude of the unemployment–vacancy correlation. Log linearization also understates the impulse responses in unemployment in recessions, but overstates the responses in the market tightness in booms. Finally, the second-order perturbation in logs can induce severe Euler equation errors, which are often much larger than those from log linearization.

Keywords. Search frictions, unemployment, projection, perturbation, nonlinear dynamics, parameterized expectations, finite elements.

JEL classification. E24, E32, J63, J64.

1. Introduction

The Diamond (1982), Mortensen (1982), and Pissarides (1985) (DMP) search model of equilibrium unemployment is the dominant framework of the labor market. A large literature has developed to address whether the model can quantitatively explain labor market volatilities.[1] More generally, the DMP model has been adopted throughout macroeconomics, including Merz (1995) and Andolfatto (1996) on business cycles, Gertler and

Nicolas Petrosky-Nadeau: nicolas.petrosky-nadeau@sf.frb.org
Lu Zhang: zhanglu@fisher.osu.edu

We have benefited from helpful comments from Hang Bai, Andrew Chen, Daniele Coen-Pirani, Steven Davis, Wouter Den Haan, Paul Evans, Lars-Alexander Kuehn, Dale Mortensen, Paulina Restrepo-Echavarria, Etienne Wasmer, Randall Wright, and other seminar participants at The Ohio State University and the 2013 North American Summer Meeting of the Econometric Society. We are particularly grateful to Benjamin Tengelsen for modifying a segment of our code that has greatly increased its speed. The co-editor and three anonymous referees deserve special thanks for extensive and insightful comments that have substantially improved the quality of the paper. Nicolas Petrosky-Nadeau thanks Stanford Institute for Economic Policy Research and the Hoover Institution at Stanford University for their hospitality. All remaining errors are our own. The views expressed in this paper are those of the authors, and do not necessarily reflect the position of the Federal Reserve Bank of San Francisco or the Federal Reserve System.

[1] Shimer (2005) argues that the unemployment volatility in the baseline DMP model is too low relative to that in the data. Hall (2005) uses sticky wages, and Mortensen and Nagypál (2007) and Pissarides (2009) use fixed matching costs to help explain this volatility puzzle. Hagedorn and Manovskii (2008) show that a calibration with small profits and a low bargaining power for workers can produce realistic volatilities.

DOI: 10.3982/QE452

Trigari (2009) on the New Keynesian model, Blanchard and Gali (2010) on monetary policy, and Petrosky-Nadeau, Zhang, and Kuehn (2015) on endogenous disasters.

Our key insight is that a globally algorithm, not a local perturbation solution, is crucial for quantifying the equilibrium properties of the DMP model. We first show the impact of nonlinear dynamics on labor market moments in Hagedorn and Manovskii (2008), who argue that the DMP model produces realistic labor market volatilities under their calibration. The (quarterly) unemployment volatility is 0.145, which is close to 0.125 in the data. However, when the model is solved accurately, the unemployment volatility is 0.258, which is about twice as large as that in the data. The unemployment–vacancy correlation is also lower in magnitude, -0.567, versus -0.724 from log linearization. Finally, the stochastic mean of the unemployment rate, 6.17%, is almost one percentage point higher than its deterministic steady state, 5.28%, from log linearization. These results cast doubt on the validity of calibration that relies exclusively on steady state relations, as well as log linearization as a solution method for the DMP model.

We also demonstrate our key insight in the model of Petrosky-Nadeau, Zhang, and Kuehn (2015), who show that a real business cycle model embedded with the DMP structure, once solved accurately, gives rise to endogenous disasters. Following the common practice in the existing literature, however, we recalibrate their model by matching its moments from log linearization to the postwar data. We then compare the moments from log linearization with those from a projection algorithm. Log linearization again understates the mean unemployment rate, 5.87% versus 10.75%, and the unemployment volatility, 0.133 versus 0.158. Log linearization also overstates the volatility of labor market tightness, 0.355 versus 0.254, as well as the magnitude of the unemployment–vacancy correlation, -0.536 versus -0.359. Finally, log linearization understates business cycle volatilities, 1.72% versus 3.26% per annum for output growth, 2.41% versus 2.60% for consumption growth, and 3.26% versus 4.45% for investment growth.

The two algorithms also differ in impulse responses. First, the unemployment responses from projection are substantially stronger in recessions than in booms. In response to a negative 1 standard deviation shock to the log productivity, the unemployment rate rises by 1.35% in the bad economy (the 5th percentile of the model's trivariate distribution of employment, capital, and log productivity), but only by 0.035% in the good economy (the 95th percentile of the trivariate distribution). This strong nonlinearity is missed by log linearization, which implies a response of only 0.327% in the bad economy. Second, the log linearization responses in the market tightness are substantially stronger in booms than in recessions. In response to a positive impulse, the market tightness jumps up by 2.38 in the good economy, but only by 0.134 in the bad economy. In contrast, the projection response is only 0.168 in the good economy.

The model's nonlinear dynamics are responsible for the differences across algorithms. Intuitively, matching frictions induce congestion externality. In recessions many unemployed workers compete for a small pool of vacancies, causing the vacancy filling rate to approach its upper limit of unity, and fail to increase further. As such, the

Hall and Milgrom (2008) replace the Nash bargaining wage with a credible bargaining wage. Finally, Petrosky-Nadeau and Wasmer (2013) use financial frictions to increase labor market volatilities.

marginal costs of hiring (inversely related to the vacancy filling rate) hardly decline, exacerbating the impact of falling profits to stifle job creation. Consequently, unemployment spikes up in recessions. In contrast, in booms many vacancies compete for a small pool of unemployed workers. The vacancy fill rate is sensitive to an extra vacancy, causing the marginal costs of hiring to rise rapidly to slow down job creation. As such, the economy expands, unemployment falls, and the market tightness rises only gradually in booms (Petrosky-Nadeau, Zhang, and Kuehn (2015)). These nonlinear dynamics are fully captured by the projection algorithm, but are largely missed by log linearization.

In the Hagedorn–Manovskii (2008) model with risk neutrality, linear production, and labor productivity as the only state, the second-order perturbation in logs improves on log linearization, but still fails to deliver accurate moments. The unemployment volatility is 0.164, which, although higher than 0.133 from log linearization, is still lower than 0.251 from projection. Similarly, the unemployment–vacancy correlation is -0.791, which is still far from -0.564 from projection. More important, in the richer model of Petrosky-Nadeau, Zhang, and Kuehn (2015) with risk aversion, nonlinear production with capital, and multiple state variables, the second-order perturbation delivers wildly inaccurate results. Because the economy often wanders far away from the deterministic steady state, the second-order coefficients calculated locally induce very large errors.

Our work suggests that many results in the prior quantitative search literature need to be reexamined with a global solution. Even for studies that use nonlinear algorithms on stylized models with risk neutrality and linear production, we show that the quality of Markov-chain approximation to the continuous productivity process matters. Because the productivity process is often calibrated to be highly persistent, the Rouwenhorst (1995) discretization delivers more accurate results than the more popular Tauchen (1986) method. More important, richer business cycle models embedded with the DMP structure have been almost exclusively solved with the low-order perturbation method in the existing literature. We show that the strong nonlinear dynamics render the perturbation method largely ineffective, if not misleading, in this class of models.

Our work also contributes to the computational economics literature. Our nonlinear algorithm is built on Judd (1992), who pioneers the projection method for solving dynamic equilibrium models. Our algorithm is also built on Christiano and Fisher (2000), who show how to incorporate occasionally binding constraints into a projection algorithm. Most prior studies compare different solution methods for the stochastic growth model and its extensions. Prominent examples include Aruoba, Fernández-Villaverde, and Rubio-Ramírez (2006), Caldara, Fernández-Villaverde, Rubio-Ramírez, and Yao (2012), and Fernández-Villaverde and Levintal (2016) for the baseline stochastic growth model, Algan, Allais, and Den Haan (2010), Den Haan and Rendahl (2010), and Maliar, Maliar, and Valli (2011) for the incomplete markets model with heterogenous agents and aggregate uncertainty, as well as Kollmann, Maliar, Malin, and Pichler (2011), Maliar, Maliar, and Judd (2011), Malin, Krueger, and Kubler (2011), and Pichler (2011) for the multicountry real business cycle model. We are not aware of any prior studies that compare solution methods for the DMP model. Most important, while prior studies find that the perturbation method is competitive in terms of accuracy with the

projection method for solving the stochastic growth model, we find the perturbation method to be inadequate for the DMP model.

Section 2 compares solution methods for solving the Hagedorn–Manovskii (2008) (HM) model. Section 3 compares the methods for solving the Petrosky-Nadeau–Zhang–Kuehn (2015) (PZK) model. Finally, Section 4 concludes.

2. The Hagedorn–Manovskii model

2.1 *Environment*

There exist a representative household and a representative firm with labor as the productive input. Following Merz (1995), we use the representative family construct, which implies perfect consumption insurance. The household has a continuum with a unit mass of members who are either employed or unemployed. The fractions of employed and unemployed workers are representative of the population at large. The household pools the income of all the members together before choosing per capita consumption and asset holdings. The household is risk neutral with a time discount factor β.

The representative firm posts a number of job vacancies, V_t, to attract unemployed workers, U_t. Vacancies are filled via a constant returns to scale matching function,

$$G(U_t, V_t) = \frac{U_t V_t}{\left(U_t^{\iota} + V_t^{\iota}\right)^{1/\iota}}, \tag{1}$$

in which $\iota > 0$ is a constant parameter. This matching function, from Den Haan, Ramey, and Watson (2000), implies that matching probabilities fall between 0 and 1.

Define $\theta_t \equiv V_t/U_t$ as the vacancy–unemployment (V/U) ratio. The probability for an unemployed worker to find a job per unit of time (the job finding rate) is

$$f_t = f(\theta_t) = \frac{G(U_t, V_t)}{U_t} = \frac{1}{\left(1 + \theta_t^{-\iota}\right)^{1/\iota}}. \tag{2}$$

The probability for a vacancy to be filled per unit of time (the vacancy filling rate) is

$$q_t = q(\theta_t) = \frac{G(U_t, V_t)}{V_t} = \frac{1}{\left(1 + \theta_t^{\iota}\right)^{1/\iota}}. \tag{3}$$

An increase in vacancies relative to unemployed workers makes it harder to fill a vacancy, $q'(\theta_t) < 0$. As such, θ_t is labor market tightness from the firm's perspective.

The firm takes aggregate labor productivity, X_t, as given. We specify $x_t \equiv \log(X_t)$ as

$$x_{t+1} = \rho x_t + \sigma \varepsilon_{t+1}, \tag{4}$$

in which $\rho \in (0, 1)$ is the persistence, $\sigma > 0$ is the conditional volatility, and ε_{t+1} is an independently and identically distributed (i.i.d.) standard normal shock. The firm uses labor to produce output, Y_t, with a constant returns to scale production technology,

$$Y_t = X_t N_t. \tag{5}$$

The representative firm incurs costs in posting vacancies with the unit cost,

$$\kappa_t = \kappa_K X_t + \kappa_W X_t^{\xi}, \tag{6}$$

in which κ_K, κ_W, and ξ are positive parameters. Once matched, jobs are destroyed at a constant rate of s per period. Employment evolves as

$$N_{t+1} = (1-s)N_t + q(\theta_t)V_t, \tag{7}$$

in which $q(\theta_t)V_t$ is the number of new hires. Because the population has a unit mass, $U_t = 1 - N_t$, N_t and U_t are also the employment and unemployment rates, respectively.

The dividends to the firm's shareholders are given by $D_t = X_t N_t - W_t N_t - \kappa_t V_t$, in which W_t is the wage rate. Taking $q(\theta_t)$ and W_t as given, the firm posts an optimal number of job vacancies to maximize the cum-dividend market value of equity, S_t, defined as $\max_{\{V_{t+\tau}, N_{t+\tau+1}\}_{\tau=0}^{\infty}} E_t[\sum_{\tau=0}^{\infty} \beta^{\tau}[X_{t+\tau}N_{t+\tau} - W_{t+\tau}N_{t+\tau} - \kappa_{t+\tau}V_{t+\tau}]]$, subject to equation (7) and a nonnegativity constraint on vacancies

$$V_t \geq 0. \tag{8}$$

Because $q(\theta_t) > 0$, this constraint is equivalent to $q(\theta_t)V_t \geq 0$. As such, the only source of job destruction is the exogenous separation of employed workers from the firm.

Let λ_t denote the multiplier on the constraint $q(\theta_t)V_t \geq 0$. From the first-order conditions with respect to V_t and N_{t+1}, we obtain the intertemporal job creation condition

$$\frac{\kappa_t}{q(\theta_t)} - \lambda_t = E_t\left[\beta\left(X_{t+1} - W_{t+1} + (1-s)\left(\frac{\kappa_{t+1}}{q(\theta_{t+1})} - \lambda_{t+1}\right)\right)\right]. \tag{9}$$

Intuitively, the marginal costs of hiring at time t (with the $V \geq 0$ constraint accounted for) equal the marginal value of a worker to the firm, which equals the marginal benefits of hiring at period $t+1$, discounted to t with the discount factor, β. The marginal benefits at $t+1$ include the marginal product of labor, X_{t+1}, net of the wage rate, W_{t+1}, plus the marginal value of a worker, which equals the marginal costs of hiring at $t+1$, net of separation. Finally, the optimal policy also satisfies the Kuhn–Tucker conditions

$$q(\theta_t)V_t \geq 0, \qquad \lambda_t \geq 0, \quad \text{and} \quad \lambda_t q(\theta_t)V_t = 0. \tag{10}$$

Equilibrium wages are determined endogenously from the sharing rule per the outcome of a generalized Nash bargaining process between the employed workers and the firm. Let $\eta \in (0,1)$ be the workers' relative bargaining weight and let b be the workers' flow value of unemployment activities. The wage rate is given by

$$W_t = \eta(X_t + \kappa_t\theta_t) + (1-\eta)b. \tag{11}$$

Let C_t denote consumption. In equilibrium, the goods market clearing condition says

$$C_t + \kappa_t V_t = X_t N_t. \tag{12}$$

2.2 *Algorithms*

To solve the model accurately, we design a projection algorithm.

Projection Because of risk neutrality and linear production, the state space of the model consists of only log productivity, x_t. Both sides of equation (9) depend only on x_t, and not on employment, N_t. This convenient property no longer holds with either risk aversion or a production function with decreasing marginal product of labor, or both. Our goal is to solve for labor market tightness, $\theta_t = \theta(x_t)$, and the multiplier function, $\lambda_t = \lambda(x_t)$ from equation (9). We must work with the job creation condition because the competitive equilibrium is not Pareto optimal. In addition, $\theta(x_t)$ and $\lambda(x_t)$ must also satisfy the Kuhn–Tucker conditions (10).

The standard projection method would approximate $\theta(x_t)$ and $\lambda(x_t)$ directly to solve the job creation condition while obeying the Kuhn–Tucker conditions. However, with the $V_t \geq 0$ constraint, these kinked functions might cause problems in the approximation with smooth basis functions. To deal with this issue, we follow Christiano and Fisher (2000) to approximate the conditional expectation in the right-hand side of equation (9) as $\mathcal{E}_t \equiv \mathcal{E}(x_t)$. A mapping from $\mathcal{E}_t$ to policy and multiplier functions then eliminates the need to parameterize the multiplier function separately. In particular, after obtaining $\mathcal{E}_t$, we first calculate $\tilde{q}(\theta_t) \equiv \kappa_t/\mathcal{E}_t$. If $\tilde{q}(\theta_t) < 1$, the nonnegativity constraint is not binding, we set $\lambda_t = 0$ and $q(\theta_t) = \tilde{q}(\theta_t)$, and then solve $\theta_t = q^{-1}(\tilde{q}(\theta_t))$, in which $q^{-1}(\cdot)$ is the inverse function of $q(\cdot)$ from equation (3). If $\tilde{q}(\theta_t) \geq 1$, the constraint is binding, and we set $\theta_t = 0$, $q(\theta_t) = 1$, and $\lambda_t = \kappa_t - \mathcal{E}_t$.

We implement both discrete and continuous state space methods. For the former, we approximate the persistent log productivity, x_t, based on the Rouwenhorst (1995) method. We use 17 grid points to cover the values of x_t, which are precisely within 4 unconditional standard deviations above and below the unconditional mean of zero. The conditional expectation in the right-hand side of equation (9) is calculated via matrix multiplication. We do not use the more popular Tauchen (1986) method because it is less accurate when the productivity process is highly persistent (Section 2.6). To obtain an initial guess of the $\mathcal{E}(x_t)$ function, we use the log-linear solution.

For the continuous state space method, we approximate the $\mathcal{E}(x_t)$ function (within 4 unconditional standard deviations of x_t from its unconditional mean of zero) with tenth-order Chebychev polynomials. The Chebychev nodes are obtained with collocation. The Miranda–Fackler (2002) CompEcon toolbox is used for function approximation and interpolation. The conditional expectation in the right-hand side of equation (9) is computed with the Gauss–Hermite quadrature (Judd (1998, pp. 261–263)).

A technical issue arises with the wide range of the state space of x_t. When x_t is sufficiently low, the conditional expectation in the right-hand side of equation (9), $\mathcal{E}_t$, can be negative. A negative $\mathcal{E}_t$ means that the firm should exit the economy, a decision that we do not model explicitly. In practice, we deal with this technical complexity by restricting simulated x_t values to be within 3.4645 unconditional standard deviations from zero. The smaller interval is precisely the range of the discrete state space with 13 grid points from the Rouwenhorst procedure. The smaller range of x_t guarantees that $\mathcal{E}_t$ is always

positive. We opt to obtain the model solution on the wider range of x_t to ensure its precision over the smaller range. In any event, the results are quantitatively similar with 13 or 17 grid points of x_t (Section 2.6).

Perturbation We implement log linearization and the second-order perturbation in logs using Dynare (Adjemian, Bastani, Juillard, Mihoubi, Perendia, Ratto, and Villemot (2011)). Because Dynare is well know, we simply report our codes in Appendix A.1. Two comments are in order. First, we ignore the vacancy nonnegativity constraint by setting the multiplier, λ_t, to be zero for all t. Doing so is consistent with the common practice in the literature. Second, following Den Haan's (2011) recommendation, we substitute out as many variables as we can, and use only a minimum number of equations in the Dynare program. We use only three equations (the employment accumulation equation, the job creation condition, and the law of motion for log productivity) with three primitive variables (employment, log productivity, and consumption). The solutions to all the other variables are obtained using the model's actual nonlinear equations, which connect all the other variables to the three variables in the perturbation system.

2.3 *Labor market moments*

It is customary to detrend variables in log deviations from the Hodrick–Prescott (1997, HP) trend with a smoothing parameter of 1600. In contrast, we use the HP-filtered cyclical component of proportional deviations from the mean with the same smoothing parameter. We cannot take logs because vacancies can be zero in simulations when the $V_t \geq 0$ constraint is binding. We use the same data sources and sample (from the first quarter in 1951 to the fourth quarter in 2004) as HM (2008, Table 3) to facilitate comparison. The seasonally adjusted unemployment is from the Current Population Survey at the Bureau of Labor Statistics (BLS). The seasonally adjusted help-wanted advertising index (a proxy for job vacancies) is from the Conference Board. Both unemployment and vacancies are quarterly averages of monthly series. The seasonally adjusted real average output per person in the nonfarm business sector (a proxy for labor productivity) is from the BLS. Using the HP-filtered cyclical components of proportional deviations from the mean, we calculate the standard deviations of unemployment, vacancy, and labor market tightness to be 0.119, 0.134, and 0.255, which are close to 0.125, 0.139, and 0.259, respectively, reported in HM's Table 3 based on log deviations. Finally, unemployment and vacancy have a correlation of -0.913, indicating a downward-sloping Beveridge curve, and the correlation is close to -0.919 in HM.

To solve and simulate from the model, we use exactly the same parameter values from HM's weekly calibration. The time discount factor, β, is $0.99^{1/12}$. The persistence of log productivity, ρ, is 0.9895, and its conditional volatility, σ, is 0.0034. The workers' bargaining weight, η, is 0.052, and their flow value of unemployment activities, b, is 0.955. The job separation rate, s, is 0.0081. The elasticity of the matching function, ι, is 0.407. Finally, for the vacancy cost function, the capital cost parameter, κ_K, is 0.474, the labor cost parameter, κ_W, is 0.11, and the exponential parameter in the labor cost, ξ, is 0.449.

Figure 1 plots the conditional expectation, $\mathcal{E}_t$, and labor market tightness, θ_t, from the discrete state space method with projection, over the range that encompasses 3.4645

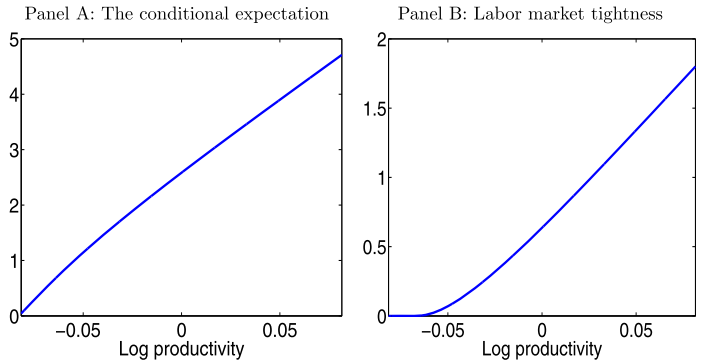

FIGURE 1. The conditional expectation and labor market tightness in the HM model. The figure plots the conditional expectation, $\mathcal{E}_t$, and labor market tightness, θ_t, solved from the discrete state space method with 17 grid points of the log productivity, x_t. The plots cover the range that encompasses 3.4645 unconditional standard deviations of x_t from zero.

unconditional standard deviations of log productivity, x_t, above and below zero. The plots from the continuous state space method are virtually identical and are omitted. The $\mathcal{E}_t$ function is smooth in x_t and θ_t also seems well behaved, although it shows a fair amount of curvature when it hits zero with low values of x_t.

To calculate labor market moments, we first reach the model's ergodic distribution by simulating the economy for $500 \times 12 \times 4$ weekly periods from the initial condition of zero for log productivity and 0.947 for employment (its deterministic steady state). From the ergodic distribution, we repeatedly simulate 5000 artificial samples, each with 648×4 weekly periods. We take the quarterly averages of the weekly unemployment, vacancy, and labor productivity to obtain 216 quarterly observations, matching HM's sample length. We then calculate the model moments for each artificial sample, and report the cross-simulation averages.

Table 1 reports labor market moments from the HM model. Panel A is identical to Table 4 in HM, and Panel B reports the log-linear results. Although the moments are not identical, the results in Panel B are largely in line with those in Panel A. The unemployment volatility, 0.133, is slightly lower than 0.145 in HM, and the volatility of labor market tightness, 0.327, is slightly higher than 0.292 in HM. However, the unemployment–vacancy correlation is −0.848, which is somewhat higher in magnitude than −0.724 in HM.[2] Panel C reports the labor market moments from the second-order perturbation in logs. Relative to log linearization, the unemployment volatility increases somewhat from 0.133 to 0.164. The volatility of labor market tightness drops from 0.327 to 0.263. Finally, the unemployment–vacancy correlation falls in magnitude from −0.848 to −0.791.

[2]As noted, because vacancies can hit zero (albeit infrequently) in the model solved with the projection algorithm, we cannot take logs. To facilitate comparison with the projection results, Panel B of Table 1 is based on HP-filtered proportional deviations from the mean. In untabulated results, we have experimented with detrending all the variables as log deviations from the HP trend as in HM (2008). (The $V_t \geq 0$ constraint is never binding with log linearization.) The unemployment volatility is 0.146, the volatility of labor market tightness is 0.284, and the unemployment–vacancy correlation is −0.777. Comparing these results with those in Panel B shows that the detrending method does not materially affect the log-linear results.

TABLE 1. Labor market moments in the HM model.

	U	V	θ	X		U	V	θ	X
	Panel A: HM (2008, Table 4)					Panel B: Log Linearization			
Standard deviation	0.145	0.169	0.292	0.013		0.133	0.144	0.327	0.013
Autocorrelation	0.830	0.575	0.751	0.765		0.831	0.681	0.783	0.760
Correlation matrix		−0.724	−0.916	−0.892	U		−0.848	−0.864	−0.927
			0.940	0.904	V			0.858	0.985
				0.967	θ				0.890
	Panel C: Second-Order Perturbation					Panel D: Projection			
Standard deviation	0.164	0.178	0.263	0.013		0.257	0.174	0.267	0.013
Autocorrelation	0.831	0.704	0.788	0.760		0.823	0.586	0.759	0.760
Correlation matrix		−0.791	−0.794	−0.795	U		−0.567	−0.662	−0.699
			0.946	0.973	V			0.890	0.909
				0.993	θ				0.996

Note: Panel A is borrowed from HM (2008, Table 4). In Panels B–D, we simulate 5000 artificial samples with 648×4 weekly observations in each sample. We take the quarterly averages of weekly unemployment U, vacancy, V, and labor productivity, X, to convert to 216 quarterly observations. Labor market tightness is denoted $\theta = V/U$. All the variables are in HP-filtered proportional deviations from the mean with a smoothing parameter of 1600. We calculate all the moments on the artificial samples and report the cross-simulation averages.

Panel D reports that the projection results differ from the perturbation results in quantitatively important ways. Most important, the unemployment volatility is 0.257, which is almost twice as large as that from log linearization, 0.133, and 60% higher than that of the second-order perturbation in logs, 0.164. Also, the unemployment–vacancy correlation is −0.567 from projection, and is substantially lower in magnitude than −0.848 from log linearization and −0.791 from the second-order perturbation. However, the market tightness volatility is 0.267, which is close to 0.263 from the second-order perturbation. In all, the low-order perturbation methods understate the unemployment volatility, but overstate the magnitude of the unemployment–vacancy correlation.

2.4 *Nonlinear dynamics*

Why does log linearization differ so much from projection? The crux is that the unemployment dynamics in the DMP model are highly nonlinear Petrosky-Nadeau, Zhang, and Kuehn (2015). In recessions, unemployment rises rapidly, whereas in booms, unemployment falls only gradually. The distribution of unemployment is highly skewed with a long right tail. With a global solution, the projection algorithm fully captures these nonlinear dynamics. In contrast, by focusing only on local dynamics around the deterministic steady state, log linearization ignores the large unemployment dynamics in recessions altogether. By missing the high unemployment rates in recessions, log linearization understates the unemployment mean and volatility, and by missing the gradual nature of expansions, log linearization overstates the market tightness volatility as well as the magnitude of the unemployment–vacancy correlation. The second-order perturbation in logs captures the nonlinear dynamics to some extent, but not nearly enough to be comparable to the global projection solution.

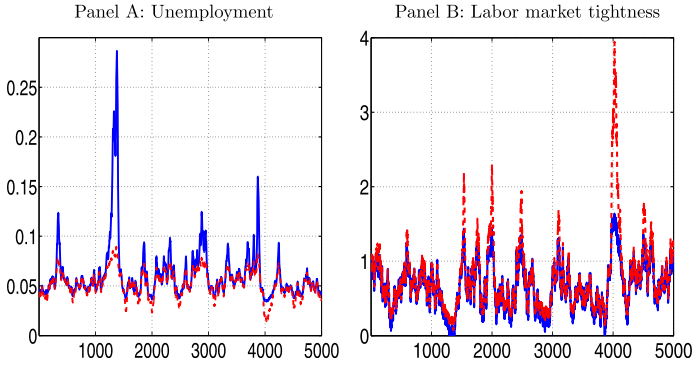

FIGURE 2. An illustrative example of simulated sample paths of unemployment and labor market tightness with identical productivity shocks, projection versus log linearization in the HM model. This figure plots the series for unemployment, U_t, and for labor market tightness, θ_t, with 5000 weekly periods. The solid line is from the projection algorithm and the broken line is from log linearization. The underlying log productivity process, x_t, is fixed across the two algorithms.

An illustrative example To illustrate the intuition, we first contrast simulated sample paths of unemployment and labor market tightness across log linearization and projection. The underlying labor productivity series is identical, and the only difference is the algorithm. Panel A of Figure 2 shows that the two unemployment sample paths differ in two critical ways. First, in recessions the unemployment rate from the projection algorithm can spike up to more than 10% (the solid line), but no such spikes are visible from the log linearization path (the broken line). For instance, in the 1379th weekly period, the unemployment rate from projection spikes up to 28.64%, whereas the unemployment rate from log linearization is only 8.67%. Second, in booms the unemployment rate from projection is often higher than that from log linearization. In particular, in the 4025th week the unemployment rate from projection reaches a low level of 3.44%. However, the unemployment rate from log linearization is even lower, 1.47%.

Panel B shows that the two market tightness series differ mostly in booms. (The two corresponding vacancy series are largely similar and are omitted to save space.) In particular, the projection-based market tightness in the 4025th week is 1.54, which is only 40% of that from log linearization, 3.83. The market tightness from log linearization often spikes up in booms, but the spikes from projection are much less visible.

Ergodic distribution Figure 3 plots unemployment, U_t, vacancy, V_t, and the labor market tightness, θ_t, against the log productivity, x_t, using 1 million weekly periods simulated from the model's ergodic distribution. From Panel A, the projection-based unemployment–productivity relation is highly nonlinear. When productivity is high, unemployment falls gradually and fluctuates within a narrow range, whereas when productivity is low, unemployment rises drastically and fluctuates within a wide range. The unemployment rate can reach above 65% in simulations. The unemployment–productivity correlation is −0.71. The simulated unemployment series is positively skewed with a long right tail. The mean unemployment rate is 6.21%, the median is

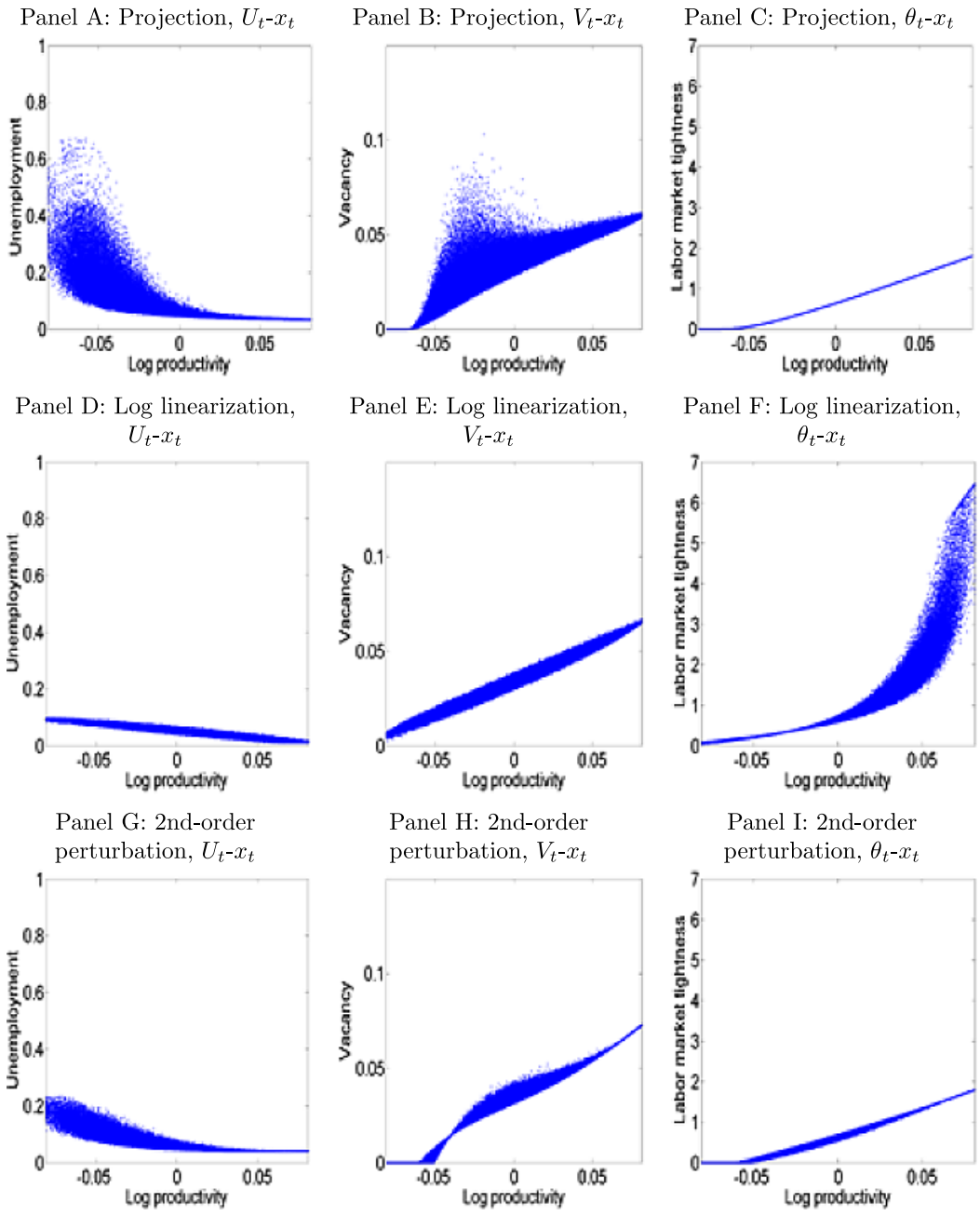

FIGURE 3. Unemployment, vacancy, and labor market tightness in simulations in the HM model. From the model's ergodic distribution based on each algorithm, we simulate 1 million weekly periods, and present the scatter plots of unemployment, U_t, vacancy, V_t, and labor market tightness, θ_t, against log labor productivity, x_t.

5.38%, the skewness is 5.19, and kurtosis is 46.84. The 2.5 percentile, 3.82%, is close to the median, whereas the 97.5 percentile is far away, 14.16%.

In contrast, Panel D shows that the unemployment–productivity relation from log linearization is virtually linear. Their correlation is nearly perfect, −0.96. The maximum unemployment in simulations is only 9.8%. The simulated unemployment series is largely symmetric. The mean unemployment is 5.28%, which is close to the median of 5.29%. The skewness is almost zero, −0.05, and the kurtosis is 2.96. The 2.5 and 97.5 percentiles, 2.72% and 7.77%, respectively, are symmetrical around the median of 5.29%. The projection-based stochastic mean unemployment rate, 6.21%, is almost 1 percentage point higher than its deterministic steady state rate, 5.28%.

From Panel G, unlike log linearization, the second-order perturbation captures some nonlinear dynamics, but not nearly as strong as projection. The unemployment–productivity correlation is −0.85, which is lower in magnitude than −0.96 from log linearization, but higher than −0.71 from projection. The maximum unemployment is 23.33%, which, although higher than 9.8% from log linearization, is lower than 67.3% from projection. The skewness of unemployment is 2.31 and the kurtosis is 11.73, both of which are smaller than those from projection, 5.19 and 46.84, respectively. However, the mean unemployment is 5.82%, which is relatively close to 6.21% from projection.

From Panels B, E, and H, the vacancy dynamics are more similar across the algorithms. The main difference is that when productivity is low, the projection-based vacancies tend to be higher than those from the perturbation methods, depending on unemployment. Intuitively, when unemployment is high and the market tightness is low, the firm posts more vacancies optimally. Because unemployment is never too high from log linearization, this effect is absent in Panel E. More important, Panels C and F show that the market tightness from log linearization is substantially higher than that from the projection algorithm in booms. As in Panel B of Figure 2, intuitively, log linearization underestimates the congestion externality in booms, thereby understating unemployment and overstating labor market tightness.

Nonlinear impulse responses To further illustrate the nonlinear dynamics of the model, we report impulse responses. We consider three different initial points: bad, median, and good economies. The bad economy is the 5th percentile of the model's bivariate distribution of employment and log productivity with projection, the median economy is the 50th percentile, and the good economy is the 95th percentile. (Although the job creation condition in equation (9) depends only on the labor productivity, other variables such as consumption, unemployment, and output also depend on the current period employment.) The unemployment rates are 10.73%, 5.37%, and 3.97%, and the log productivity levels are −0.0387, 0, and 0.0383, across the bad, the median, and the good economies, respectively. We calculate the responses to a 1 standard deviation shock to the log productivity, both positive and negative, starting from a given initial point. The impulse responses are averaged across 5000 simulations, each with 480 weeks.

Figure 4 reports the impulse responses. Several nonlinear patterns emerge. First, the responses from the projection algorithm are clearly stronger in recessions than those in booms. For instance, in response to a negative impulse, the unemployment rate shoots

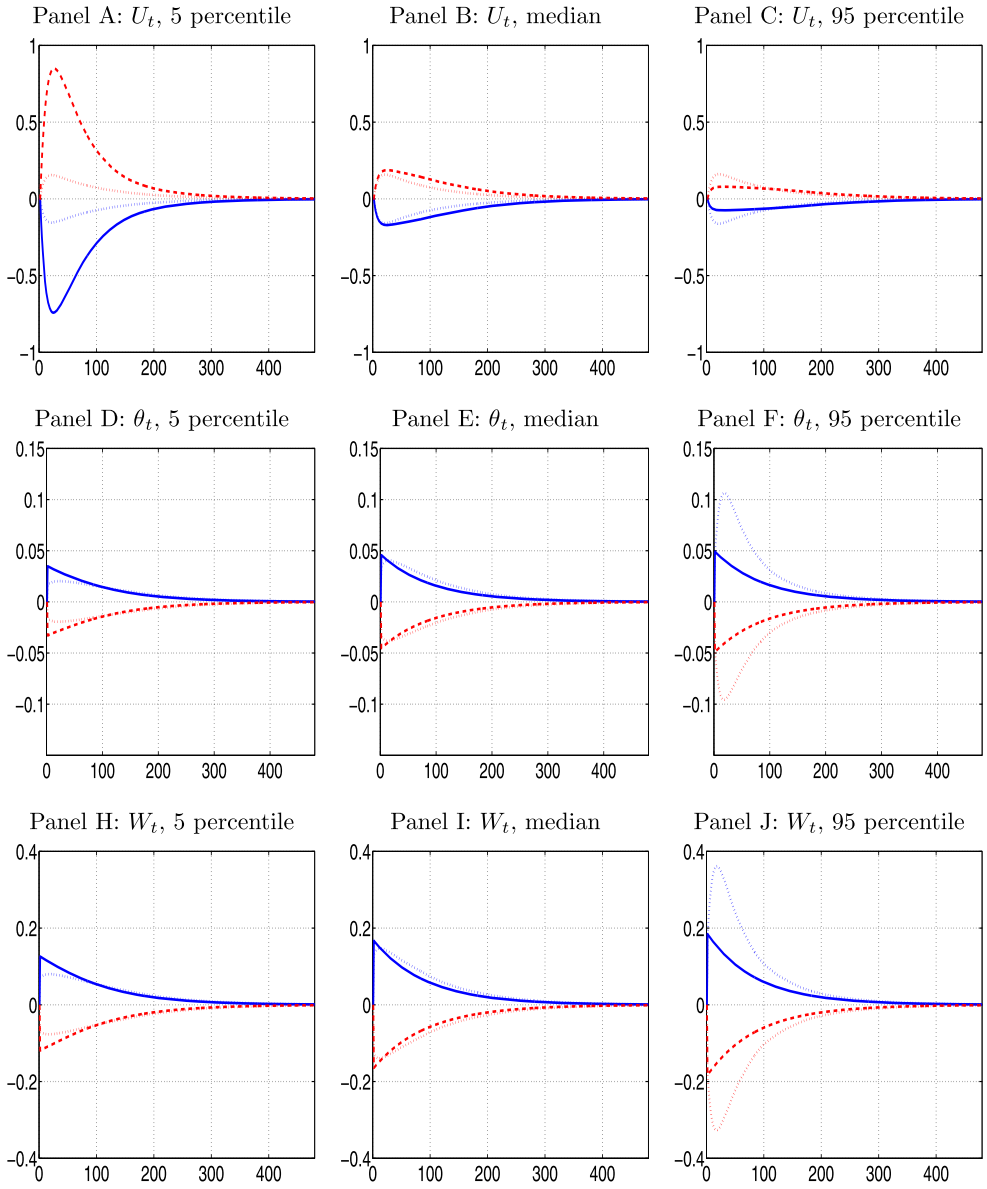

FIGURE 4. Nonlinear impulse responses in the HM model. The solid (broken) lines are the projection responses to a positive (negative) 1 standard deviation shock to the log productivity. The dotted lines are the corresponding responses from log linearization. The responses in unemployment, U_t, are changes in levels times 100, those in the market tightness, θ_t, are changes in levels, and those in wages, W_t, are changes in levels (in percent) scaled by the pre-impulse level.

up by 0.85% in the bad economy (Panel A). In contrast, the response is only 0.08%, which is an order of magnitude smaller, in the good economy (Panel C). The response in the median economy is 0.19%, which is closer to that in the good economy than that in the bad economy (Panel B). Second, and more important, although close in the median

economy, the responses in unemployment from log linearization diverge significantly from the projection responses in recessions and in booms. In particular, the responses from log linearization are substantially weaker in the bad economy. The response to a negative impulse under log linearization is 0.15%, which is less than 20% of the projection response, 0.85%. However, in the good economy, the log linearization responses are somewhat stronger than the projection responses. The log linearization response to a negative impulse is 0.16%, which is twice as large as the projection response, 0.08%. Third, the responses in the market tightness are largely similar in the bad and the median economies across the two algorithms (Panels D and E). However, the projection responses are only about one-half of those from log linearization (Panel F). Intuitively, log linearization understates the congestion externality and the gradual nature of expansions, but the effect can be fully captured by the projection algorithm. Finally, wages are inertial. In the bad economy, in response to a negative impulse, wages drop by only about 0.12% relative to its pre-impulse level in the projection solution (Panel H). This percentage drop in wages is even lower than that in the good economy, 0.18% (Panel J). Relative to projection, log linearization understates the percentage drop in the bad economy to be 0.08%, but overstates that in the good economy to be 0.33%.

2.5 *Accuracy tests*

While it is natural to expect that projection would be more accurate than log linearization, we are not aware of any prior attempt to quantify the errors for log linearization relative to projection in the DMP model. We fill this gap.

Following Judd (1992), we calculate Euler equation errors, defined as

$$e_t \equiv E_t\left[\beta\left(X_{t+1} - W_{t+1} + (1-s)\left(\frac{\kappa_{t+1}}{q_{t+1}} - \lambda_{t+1}\right)\right)\right] - \left(\frac{\kappa_t}{q_t} - \lambda_t\right). \tag{13}$$

Judd suggests unit-free residuals as percentage deviations from optimal consumption. However, this calculation involves taking the inverse of the marginal utility function and is infeasible in the HM model because of linear utility. As such, we use the regular residuals. If an algorithm is accurate, e_t should be zero on all points in the state space.

We calculate the errors on a fine log productivity–employment grid. We put the grid on employment, N_t, besides the log productivity, because the perturbation errors depend on employment. We create an evenly spaced grid that consists of 1000 points of x_t and 1000 points of N_t. For projection, we use cubic splines to interpolate the conditional expectation function, $\mathcal{E}(x_t)$, for the x_t values that are not on its original 17-point discrete state space. To calculate the conditional expectation in equation (13) accurately, we use the Gauss–Hermite quadrature with 5 nodes (the results from the 10-node quadrature are quantitatively similar).

Panel A of Figure 5 shows that the projection algorithm offers an accurate solution to the model. The errors are in the magnitude of 10^{-4}. In contrast, Panel B shows that log linearization exhibits large approximation errors that are 3–4 orders of magnitudes larger than the projection errors. In particular, the log linearization errors vary from

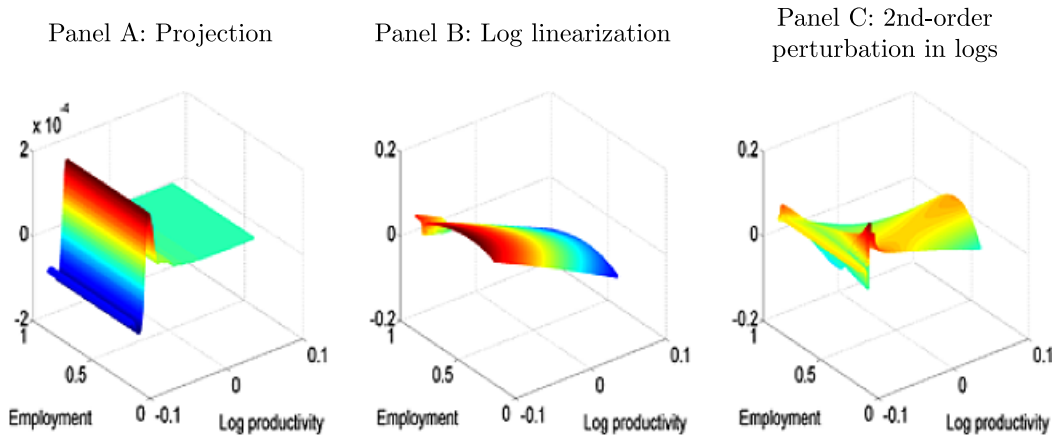

FIGURE 5. Euler equation errors in the state space in the HM model. This figure plots the Euler equation errors on the log productivity–employment grid.

−11.5% to 7.13%. From Panel C, the second-order perturbation in logs can be less accurate than log linearization. At the deterministic steady state, the error is close to that from log linearization. However, the errors can be larger once the economy wanders away from the steady state. The errors vary from −13.88% to 13.34%, and the extreme errors are larger than those from log linearization.

We also calculate Euler equation errors from the model's ergodic distribution from a given algorithm. For projection, we use the policy function from the 17-point discrete state space. We simulate from the continuous state space and use cubic splines to interpolate the conditional expectation function for the x_t values that are not on the original 17-point grid. To calculate the conditional expectation accurately in simulations, we use the Gauss–Hermite quadrature. Further accuracy tests based on alternative designs are reported in Section 2.6. Figure 6 shows the histograms of the errors, e_t, defined in equation (13), based on 1 million weekly periods. From Panel A, the projection errors are extremely small. The mean error is 2.22×10^{-6}, the mean absolute error is 6.84×10^{-6}, and the maximum absolute error is 1.5×10^{-4}. In addition, the 2.5th, 50th, and 97.5th percentiles of the errors are 1.22×10^{-4}, 4.9×10^{-6}, and 4.9×10^{-6}. In contrast, Panel B shows large errors for log linearization. The mean error is −3.69%, the mean absolute error is 3.75%, and the maximum absolute error is 11.5%. Also, the 2.5th, 50th, and 97.5th percentiles of the errors are −11.06%, −3.66%, and −8.76%. The deterministic steady state consumption is 0.927. As such, the log linearization errors are economically large. Finally, Panel C shows that the errors from the second-order perturbation in logs are quantitatively similar to those from log linearization.

2.6 *The quality of Markov-chain approximations*

HM (2008) in fact use a global algorithm to solve their model. In this subsection, we examine why their results differ from those from our global algorithm. The crux is that while we use the Rouwenhorst (1995) discretization to approximate the persistent log

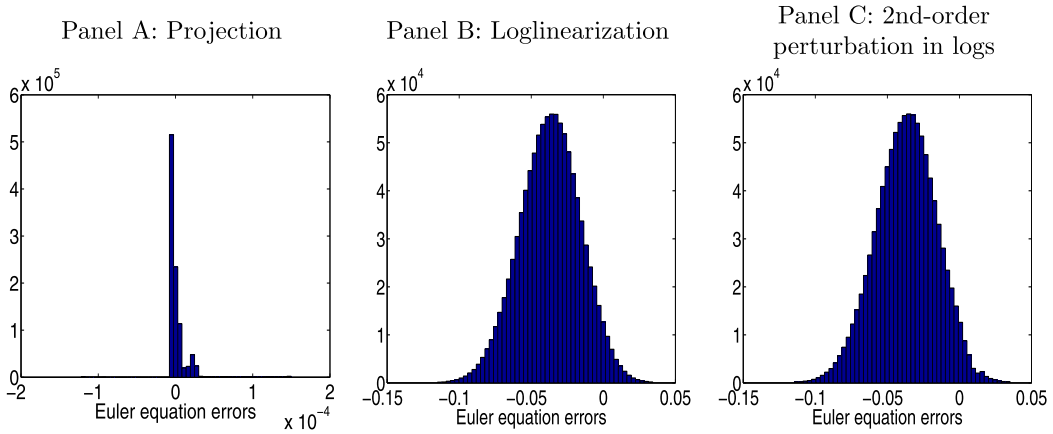

FIGURE 6. Euler equation errors in simulations in the HM model. We simulate 1 million weeks from the model's ergodic distribution based on each algorithm and plot the histograms for the Euler residuals. The underlying log productivity series, x_t, is identical across the three panels, which differ only in the algorithm.

productivity process, HM use the Tauchen (1986) discretization. This difference goes a long way to reconcile our results with theirs. In particular, we show that (i) the results from the Rouwenhorst method are very close to those from the continuous state space method, (ii) the results from the Rouwenhorst method are robust to a sufficient number of grid points, and (iii) the results from the Tauchen method are quite sensitive to the grid boundaries.

Quantitative results Table 2 reports labor market moments under alternative Markov-chain approximations. Panel A reports the results from the continuous state space method. The unemployment volatility is 0.259, the market tightness volatility is 0.268, and the unemployment–vacancy correlation is −0.567, all of which are very close to 0.257, 0.267, and −0.567, respectively, from the Rouwenhorst method with 17 grid points (Panel B, same as Panel D in Table 1).[3] The results from the Rouwenhorst discretization are robust to the number of grid points. Panel C uses 13 grid points that cover a range of the log productivity that is 3.4645 unconditional standard deviations from zero. The unemployment volatility is 0.254, the volatility of labor market tightness is 0.268, and the unemployment–vacancy correlation is −0.572, which are close to 0.257, 0.267, and −0.567, respectively, with 17 grid points (Panel B).

[3]As noted, the Rouwenhorst grid with 17 points encompasses a wide range of 4 unconditional standard deviations of the log productivity above and below its unconditional mean of zero. We simulate the log productivity from the continuous state space, and restrict the simulated values to be within 3.4645 unconditional standard deviations from zero. However, simulating from the discrete state space with 17 grid points yields quantitatively similar results. The unemployment volatility is 0.253, the market tightness volatility is 0.267, and the unemployment–vacancy correlation is −0.570 (untabulated). In Panels C–F of Table 2, we simulate directly from the (smaller) discrete state spaces because the conditional expectation is always positive.

TABLE 2. Labor market moments under alternative approximations to the persistent productivity process.

	U	V	θ	X		U	V	θ	X
	Panel A: Continuous State Space					Panel B: Rouwenhorst, $n_x = 17$			
Standard deviation	0.259	0.175	0.268	0.013		0.257	0.174	0.267	0.013
Autocorrelation	0.823	0.586	0.760	0.760		0.823	0.586	0.759	0.760
Correlation matrix		−0.567	−0.662	−0.698	U		−0.567	−0.662	−0.699
			0.890	0.909	V			0.890	0.909
				0.996	θ				0.996
	Panel C: Rouwenhorst, $n_x = 13$					Panel D: Rouwenhorst, $n_x = 5$			
Standard deviation	0.254	0.175	0.268	0.013		0.219	0.172	0.267	0.013
Autocorrelation	0.827	0.583	0.759	0.760		0.830	0.581	0.760	0.760
Correlation matrix		−0.572	−0.669	−0.704	U		−0.608	−0.716	−0.744
			0.891	0.908	V			0.901	0.914
				0.997	θ				0.998
	Panel E: Tauchen, $m = 2$					Panel F: Tauchen, $m = 3.4645$			
Standard deviation	0.154	0.149	0.246	0.013		0.299	0.192	0.286	0.014
Autocorrelation	0.813	0.582	0.749	0.747		0.825	0.580	0.759	0.760
Correlation matrix		−0.697	−0.825	−0.842	U		−0.535	−0.625	−0.669
			0.930	0.936	V			0.876	0.899
				0.997	θ				0.995

Note: Results are averaged across 5000 samples from each approximation with the projection algorithm. The number of grid points for the log productivity in the Rouwenhorst discretization is denoted n_x. When implementing the Tauchen discretization, we use 35 grid points, but vary the boundaries of the grid in terms of the number of unconditional standard deviations, denoted m, from the unconditional mean of zero. The simulation design is identical to Table 1.

Panel D reports the results from the 5-point Rouwenhorst grid that covers 2 unconditional standard deviations above and below zero. This range is comparable with the HM implementation of the Tauchen method that also covers 2 standard deviations above and below from zero. Even with only 5 grid points, the unemployment volatility is 0.219, which is not far from 0.257 with 17 grid points. The market tightness volatility is 0.267, which is identical to that from the larger grid. Finally, the unemployment–vacancy correlation is −0.608 relative to −0.567 from the 17-point grid.

Panels E and F show that the results from the Tauchen discretization are quite sensitive to the range of the grid chosen. Unlike the Rouwenhorst procedure, in which the number of grid points automatically determines the range of the grid, the Tauchen method allows a separate parameter to pin down the grid range, regardless of the number of grid points. We always use 35 grid points as in HM, but experiment with two different ranges that cover 2 and 3.4645 unconditional standard deviations of the log productivity from zero. From Panel E, with the smaller range as in HM, the results from the Tauchen method are largely in line with those reported in their Table 4 (see Panel A of our Table 1). The unemployment volatility is 0.154, the market tightness volatility is 0.246, and the unemployment–vacancy correlation is −0.697, which are (relatively) close to 0.145, 0.292, and −0.724, respectively, in HM.

Panel F shows that enlarging the range of the Tauchen grid raises the unemployment volatility, but dampens the unemployment–vacancy correlation. When the range increases from 2 to 3.4645 unconditional standard deviations from zero, the unemployment volatility rises from 0.154 to 0.299, and the unemployment–vacancy correlation falls in magnitude from −0.697 to −0.535. The market tightness volatility also increases somewhat from 0.246 to 0.286. The only difference between Panels E and F is the range parameter of the Tauchen grid. As such, these results cast doubt on the Tauchen method, but lend support to the Rouwenhorst method in approximating highly persistent autoregressive processes.[4]

Euler equation errors Figure 7 reports the Euler residuals from the model's ergodic distribution based on a given approximation procedure of the continuous log productivity process, x_t. In Panel A, we use the policy function approximated with the 10-order Chebychev polynomials, which are in turn used to interpolate the policy rule on the simulated x_t values that are not directly on the original Chebychev nodes. The Euler residuals are largely comparable with those from the discrete Rouwenhorst method with 17 grid points. In particular, the mean error, the mean absolute error, and the maximum absolute error are -7.76×10^{-7}, 2.02×10^{-5}, and 1.51×10^{-4}, which are close to 2.22×10^{-6}, 6.84×10^{-6}, and 1.5×10^{-4}, respectively, from our benchmark discrete state space method. Panels B–E report the Euler residuals from alternative Markov-chain approximation to the continuous x_t process. Across all the remaining panels, we simulate from the continuous state space, and use cubic splines to interpolate the policy function solved on a given discrete state space on the simulated x_t values that are not on the grid. To calculate the conditional expectation accurately, we use the Gauss–Hermite quadrature (same in Panel A).

Panel B shows that the Rouwenhorst procedure with 13 grid points is fairly accurate. The mean error is 2.99×10^{-6}, the mean absolute error is 9.19×10^{-6}, and the maximum absolute error is 1.73×10^{-4}. However, Panel C shows that using only 5 grid points in the Rouwenhorst procedure is very inaccurate, with a mean (absolute) error of 2.79 and a maximum absolute error of 5.1. From Panel D, the Tauchen method with $m = 2$ (the boundaries of the grid in terms of the number of unconditional standard deviations of x_t) leaves much to be desired. Although the mean error is only -9.09×10^{-5}, the mean absolute error is 0.11% and the maximum absolute error 18.4%. Finally, Panel E shows that the Tauchen method with $m = 3.4645$ improves on $m = 2$ greatly, with a mean absolute error of 5.39×10^{-5}. However, the maximum absolute error is 0.68%, which is more than 1 order of magnitude larger than 1.5×10^{-4} from our benchmark Rouwenhorst method with 17 grid points.

3. The Petrosky-Nadeau–Zhang–Kuehn model

In this section, we explore how projection deviates from log linearization in a real business cycle model with both labor search frictions and capital accumulation.

[4] Kopecky and Suen (2010) also note that the performance of the Tauchen (1986) method is extremely sensitive to the choice of the free parameter that determines the range of the discrete state space. Their results are based on the stochastic growth model. We echo their conclusion in the context of the DMP model.

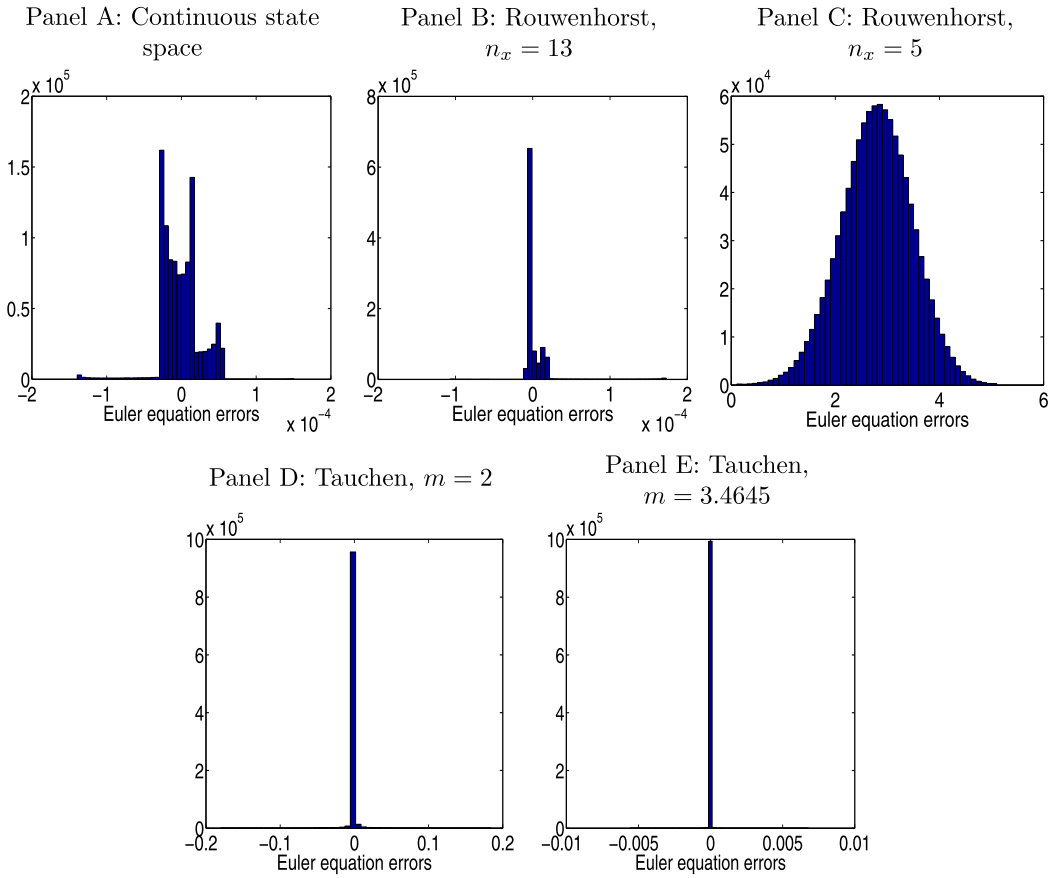

FIGURE 7. Further results on Euler equation errors in simulations in the HM model. We simulate 1 million weeks from the model's ergodic distribution based on each approximation of the continuous log productivity process, and plot the histograms for the Euler residuals. The underlying log productivity series, x_t, is identical across all the panels (and is the same series as in Figure 6). All the panels use the projection algorithm, but differ in the approximation procedure of x_t.

3.1 *Environment*

There exists a representative household with log utility, $\log(C_t)$, and its stochastic discount factor is $M_{t+1} = \beta(C_t/C_{t+1})$, in which C_t is consumption. A representative firm uses labor, N_t, and capital, K_t, to produce with a constant returns to scale technology

$$Y_t = X_t K_t^{\alpha} N_t^{1-\alpha}, \tag{14}$$

in which $\alpha \in (0, 1)$ is capital's weight. The log productivity, $x_t = \log(X_t)$, follows

$$x_{t+1} = (1-\rho)\bar{x} + \rho x_t + \sigma\varepsilon_{t+1}, \tag{15}$$

in which $\bar{x}$ is the unconditional mean of x_t. We rescale $\bar{x}$ to make the average simulated marginal product of labor around one to ease interpretation of parameter values.

The firm posts vacancies, V_t, to attract unemployed workers, U_t. The matching function is given by equation (1). We continue to impose the nonnegativity constraint on vacancies. When posting vacancies, the firm incurs the constant unit cost of κ. The firm also invests, and incurs adjustment costs when doing so. Capital accumulates as

$$K_{t+1} = (1-\delta)K_t + \Phi(I_t, K_t), \tag{16}$$

in which δ is the depreciation rate and I_t is investment. The installation function is

$$\Phi(I_t, K_t) = \left[a_1 + \frac{a_2}{1-1/\nu}\left(\frac{I_t}{K_t}\right)^{1-1/\nu}\right]K_t, \tag{17}$$

in which $\nu > 0$ is the supply elasticity of capital. We set $a_1 = \delta/(1-\nu)$ and $a_2 = \delta^{1/\nu}$ to ensure no adjustment costs in the deterministic steady state (Jermann (1998)).

The equilibrium wage, W_t, follows

$$W_t = \eta\left[(1-\alpha)\frac{Y_t}{N_t} + \kappa\theta_t\right] + (1-\eta)b, \tag{18}$$

in which the marginal product of labor is given by $(1-\alpha)Y_t/N_t$. The dividends to the firm's shareholders are given by $D_t \equiv Y_t - W_t N_t - \kappa V_t - I_t$. Taking $q(\theta_t)$ and W_t as given, the firm chooses an optimal number of vacancies and optimal investment to maximize the present value of all future dividends, subject to equations (7) and (16), as well as the vacancy nonnegativity constraint. In equilibrium, the market clearing condition says

$$C_t + I_t + \kappa V_t = Y_t. \tag{19}$$

Optimality conditions include the intertemporal job creation condition

$$\frac{\kappa}{q(\theta_t)} - \lambda_t = E_t\left[M_{t+1}\left((1-\alpha)\frac{Y_{t+1}}{N_{t+1}} - W_{t+1} + (1-s)\left(\frac{\kappa}{q(\theta_{t+1})} - \lambda_{t+1}\right)\right)\right] \tag{20}$$

and the investment Euler equation

$$\frac{1}{a_2}\left(\frac{I_t}{K_t}\right)^{1/\nu} = E_t\left[M_{t+1}\left(\alpha\frac{Y_{t+1}}{K_{t+1}} + \frac{1}{a_2}\left(\frac{I_{t+1}}{K_{t+1}}\right)^{1/\nu}(1-\delta+a_1) + \frac{1}{\nu-1}\frac{I_{t+1}}{K_{t+1}}\right)\right], \tag{21}$$

as well as the Kuhn–Tucker conditions in equation (10).[5]

3.2 *Algorithms*

Because of its disaster dynamics (PZK (2015)), the projection algorithm for the PZK model is challenging. Also, risk aversion and nonlinear production function imply that the model has three separate state variables: employment, N_t, capital, K_t, and

[5]Under our benchmark calibration (Section 3.3), the vacancy nonnegativity constraint is never binding. Intuitively, capital provides a buffer to negative shocks so that vacancy does not fall to zero. As such, zero vacancies are specific to the Hagedorn–Manovskii (2008) model with linear utility and no capital in production.

log productivity, x_t. We solve for the optimal vacancy function, $V(N_t, K_t, x_t)$, the multiplier function, $\lambda(N_t, K_t, x_t)$, and the optimal investment function, $I(N_t, K_t, x_t)$, from the intertemporal job creation condition in equation (20) and the investment Euler equation (21). The policy functions must also satisfy the Kuhn–Tucker conditions in equation (10). Because optimal investment is always positive, we approximate $I(N_t, K_t, x_t)$ directly. The positive investment is a result of the installation function in equation (17). In particular, when investment goes to zero, the marginal benefit of investment, $\partial\Phi(I_t, K_t)/\partial I_t = a_2(I_t/K_t)^{-1/\nu}$, goes to infinity. Finally, to impose the vacancy nonnegativity constraint, we continue to parameterize the conditional expectation in the right-hand side of equation (20), denoted $\mathcal{E}_t \equiv \mathcal{E}(N_t, K_t, x_t)$.

Following the recommendation of Fernández-Villaverde, Rubio-Ramírez, and Schorfheide (2016), we discretize the log productivity, x_t, with the Rouwenhorst procedure with 17 grid points.[6] The discrete state space simplifies the computation of conditional expectations to matrix multiplication, and alleviates the curse of dimensionality.

We approximate $I(N_t, K_t, x_t)$ and $\mathcal{E}(N_t, K_t, x_t)$ on each grid point of x_t. Our primary concern is with accuracy, not running time. We use the finite element method with cubic splines on 100 nodes on the employment space, $N_t \in [0.225, 0.975]$, and 100 nodes on the capital space, $K_t \in [10, 42.5]$. We take the tensor product of N_t and K_t for each grid point of x_t. We use the Miranda–Fackler CompEcon toolbox extensively for function approximation and interpolation. With two functional equations on the 17-point x_t grid, the 100-point N_t grid, and the 100-point K_t grid, we need to solve a system of 340,000 nonlinear equations. The traditional Newton-style methods are infeasible for such a large system. Following the recommendation of Judd, Maliar, Maliar, and Valero (2014), we use derivative-free fixed-point iteration with a damping parameter of 0.025. The convergence criterion is set to be 10^{-10} for the maximum absolute value of the Euler equation errors across the nonlinear equations.

To obtain a good initial guess, we proceed sequentially. We first use the log-linear solution as the initial guess on a small grid with only 5 points for employment and for capital. The initial grid only covers a small interval of employment from 0.9 to 0.975 and a small interval of capital from 30 to 40. We always use the 17-point grid for the log productivity. Upon convergence, we use the projection solution as the new initial guess. We then gradually expand the employment and capital grids by adding more grid points, reducing the lower bounds for employment and capital, and raising the upper bound for capital. We make sure that the grid bounds are binding in simulations no more than 0.02% of the time. In practice, the Newton-style methods are efficient for solving the system of nonlinear equations when the number of grid points is below 20 for employment and for capital, but quickly become infeasible afterward. With more grid points, we switch to derivative-free fixed-point iteration.

With the calibrated parameter values (Section 3.3), the deterministic steady state of employment is 0.943, and that of capital is 35.3. In simulations, the boundaries of the employment and capital spaces are rarely binding. Figure 8 reports the conditional

[6] Fernández-Villaverde, Rubio-Ramírez, and Schorfheide (2016, p. 78) write that "discretization of state variables such as the productivity shock is more often than not an excellent strategy to deal with multidimensional problems: simple, transparent, and not too burdensome computationally."

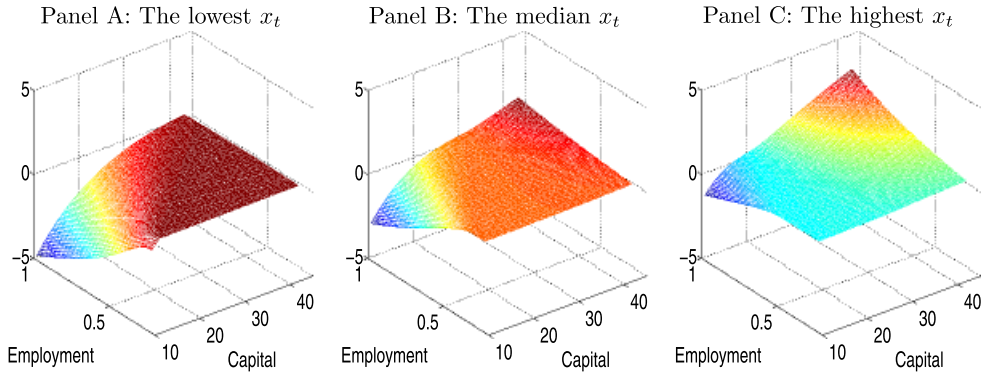

FIGURE 8. The conditional expectation function on the state space in the PZK model. This figure plots the conditional expectation function, $\mathcal{E}(N_t, K_t, x_t)$, on the employment–capital grid, N_t–K_t, for three values of the log productivity, x_t, including the lowest, median, and highest grid points in the 17-point grid of x_t.

expectation function on the N_t–K_t space for the lowest, median, and highest values of x_t on its 17-point grid. The function seems relatively smooth. In any event, we use the finite element method with cubic splines to ensure accuracy. Finally, although the conditional expectation can be negative in some regions of the large state space, it is always positive in simulations. The minimum value of $\mathcal{E}(N_t, K_t, x_t)$ in simulations is around 0.4.

We implement the log-linear solution and the second-order perturbation in logs again using Dynare (see the Dynare codes in Appendix A.2). We again ignore the vacancy nonnegativity constraint, setting $\lambda_t = 0$ for all t, and substitute out as many variables as possible to use only a minimum number of equations. We use six primitive variables (employment, capital, log productivity, consumption, investment, and labor market tightness, θ_t) with six equations (the employment accumulation equation, the capital accumulation equation, the intertemporal job creation condition, the investment Euler equation, the law of motion for the log productivity, and the definition of θ_t as the vacancy-to-unemployment ratio).

3.3 *Calibration with the log-linear solution*

Mimicking the common practice in the business cycle literature, we calibrate the model by matching its log-linear moments to the postwar U.S. data. To show the importance of different solution algorithms, we then compare the log-linear moments with those from the projection solution as well as those from the second-order perturbation in logs.

We obtain real output (gross domestic product), consumption (personal consumption expenditures), and investment (gross private domestic investment) from Table 1.1.6 in the National Income and Product Account (NIPA). Table 3 shows that the volatility of log output growth is 2.17% per annum from 1951 to 2014, the log consumption growth volatility is 1.78%, and the log investment growth volatility is 8.93%. The first-order autocorrelations of the output, consumption, and investment growth rates are 0.15, 0.34, and 0.02, respectively.

TABLE 3. Business cycle moments, data, and the PZK model.

	σ_Y	ρ_1^Y	ρ_2^Y	ρ_3^Y	ρ_4^Y	σ_C	ρ_1^C	ρ_2^C	ρ_3^C	ρ_4^C
Data	1.78	0.34	0.07	−0.05	0.06	2.17	0.15	0.01	−0.06	0.02
Log linearization	1.72	0.19	−0.07	−0.06	−0.06	2.41	0.18	−0.08	−0.07	−0.07
Second-order perturbation	3.08	0.23	−0.07	−0.07	−0.06	8.38	0.18	−0.12	−0.09	−0.07
Projection	3.26	0.21	−0.08	−0.06	−0.06	2.60	0.23	−0.06	−0.05	−0.05
	σ_I	ρ_1^I	ρ_2^I	ρ_3^I	ρ_4^I	$E[U]$				
Data	8.93	0.02	−0.16	−0.19	−0.10	5.87				
Log linearization	3.26	0.16	−0.11	−0.09	−0.08	5.75				
Second-order perturbation	5.65	0.20	−0.10	−0.09	−0.07	16.40				
Projection	4.45	0.19	−0.10	−0.08	−0.07	10.75				

Note: The volatilities (in percent) of the log output, consumption, and investment growth rates are denoted σ_Y, σ_C, and σ_I, and ρ_j^Y, ρ_j^C, and ρ_j^I are their jth-order autocorrelations, respectively; $E[U]$ is the mean unemployment rate in percent. The annual real output, consumption, and investment data are from the NIPA Table 1.1.6, and the monthly seasonally adjusted unemployment rates are from the BLS. The sample is from 1951 to 2014. For the model's results, we simulate 5000 samples from each solution of the model, time–aggregate monthly output, consumption, and investment to annual series, and we report cross-simulation averages as the model moments.

For labor market moments, we follow the sample construction in Petrosky-Nadeau and Zhang (2013). The sample is from 1951 to 2014. The monthly seasonally adjusted civilian unemployment rate series is from the BLS. We construct the vacancy rate series by drawing from four different sources of U.S. job openings: (i) the Metropolitan Life Insurance company help-wanted advertising index in newspapers from January 1951 to December 1959 from the National Bureau of Economic Research (NBER) macrohistory files; (ii) the Conference Board help-wanted index from January 1960 to December 1994; (iii) the Barnichon (2010) composite print and online help-wanted index from January 1995 to November 2000; and (iv) the seasonally adjusted job openings from December 2000 to December 2014 from the Job Openings and Labor Turnover Survey released by the BLS. To convert the help-wanted index to a vacancy rate series, we use the monthly civilian labor force over 16 years of age from the Current Employment Statistics released by the BLS. Table 3 shows that the mean unemployment rate is 5.87%. Table 4 shows that the unemployment volatility is 0.132 and the volatility of labor market tightness is 0.263. The unemployment–vacancy correlation is −0.887 and the correlation between unemployment and labor productivity is only −0.158.

As noted, we calibrate the log-linear model to the postwar U.S. data. The calibration is in monthly frequency. We use conventional values for the time discount factor, $\beta = 0.99^{1/3}$, the persistence of log productivity, $\rho_x = 0.95^{1/3}$, the capital's weight, $\alpha = 1/3$, the depreciation rate, $\delta = 0.01$, and the separation rate, $s = 0.035$. The elasticity of the matching function, ι, is 1.25, which is close to that in Den Haan, Ramey, and Watson (2000). Following Gertler and Trigari (2009), we choose the conditional volatility of the log productivity, σ, to match the output growth volatility in the data. This procedure yields $\sigma = 0.0065$, which implies an output volatility of 2.41% per annum in the model, relative to 2.17% in the data. Following PZK (2015), we choose the elasticity in the installation function, $\nu = 2$, such that the consumption growth volatility in the model is

TABLE 4. Labor market moments, data, and the PZK model.

	U	V	θ	Y/N		U	V	θ	Y/N
	Panel A: Data					Panel B: Log Linearization			
Standard deviation	0.132	0.134	0.263	0.012		0.133	0.167	0.355	0.011
Autocorrelation	0.901	0.909	0.881	0.773		0.815	0.537	0.759	0.746
Correlation matrix		−0.887	−0.830	−0.158	U		−0.536	−0.696	−0.881
			0.930	0.350	V			0.566	0.782
				0.240	θ				0.821
	Panel C: Second-Order Perturbation					Panel D: Projection			
Standard deviation	0.238	1.222	0.770	0.031		0.158	0.158	0.254	0.010
Autocorrelation	0.852	0.611	0.720	0.779		0.844	0.588	0.763	0.657
Correlation matrix		0.061	−0.153	0.346	U		−0.359	−0.473	−0.337
			0.859	0.795	V			0.899	0.983
				0.692	θ				0.930

Note: Panel A is based on postwar U.S. data from 1951 to 2014. In Panels B–D, we simulate 5000 artificial samples with 768 months in each sample. We take the quarterly averages of monthly unemployment U, vacancy, V, and labor productivity, Y/N, to convert to 256 quarters. Labor market tightness is denoted $\theta = V/U$. All the variables are in HP-filtered proportional deviations from the mean with a smoothing parameter of 1600. The model moments are cross-simulation averages.

1.72%, which is close to 1.78% in the data. However, the investment growth volatility is only 3.26%, in contrast to 8.93% in the data.

We calibrate the remaining labor market parameters in the spirit of HM (2008). The workers' bargaining weight, η, is 0.04, the flow value of unemployment activities, b, is 0.95, and the cost of vacancy posting, κ, is 0.45. These values imply an average unemployment rate of 5.75% in the model, which is close to 5.87% in the data, and an unemployment volatility of 0.133, which is close to 0.132 in the data. However, the market tightness volatility is 0.355, which is higher than 0.263 in the data. In addition, the unemployment–vacancy correlation is −0.536, which is smaller in magnitude than −0.887 in the data, and the unemployment–labor productivity correlation is −0.881, which is substantially higher than −0.158 in the data. The weakness of the DMP model in matching correlations in the data is also present in HM.

3.4 *Accuracy tests*

Before discussing how the projection moments differ from the perturbation moments, we present accuracy tests to show that the projection algorithm is accurate, log linearization is inaccurate, and the second-order perturbation is wildly incorrect.

Following Judd (1992), we use unit-free residuals in the unit of optimal consumption. Combining the stochastic discount factor with log utility, $M_{t+1} = \beta(C_t/C_{t+1})$, with equations (20) and (21) yields the unit-free job creation equation errors, denoted e_t^V, as

$$e_t^V \equiv \left[\left(\frac{\kappa}{q(\theta_t)} - \lambda_t\right) \Big/ \left(E_t\left[\frac{\beta}{C_{t+1}}\left((1-\alpha)\frac{Y_{t+1}}{N_{t+1}} - W_{t+1} + (1-s)\left(\frac{\kappa}{q(\theta_{t+1})} - \lambda_{t+1}\right)\right)\right]\right) - C_t\right] \Big/ C_t, \tag{22}$$

as well as the unit-free investment Euler equation errors, denoted e_t^I, as

$$e_t^I \equiv \left[\left(\frac{1}{a_2}\left(\frac{I_t}{K_t}\right)^{1/\nu}\right)\Big/\left(E_t\left[\frac{\beta}{C_{t+1}}\left(\alpha\frac{Y_{t+1}}{K_{t+1}} + \frac{1}{a_2}\left(\frac{I_{t+1}}{K_{t+1}}\right)^{1/\nu}(1-\delta+a_1) + \frac{1}{\nu-1}\frac{I_{t+1}}{K_{t+1}}\right)\right]\right) - C_t\right]\Big/C_t. \tag{23}$$

Because of our large, three-dimensional state space, N_t–K_t–x_t, a significant portion of the state space is never visited in simulations even with our projection algorithm. As such, we focus on the Euler residuals in simulations because only these errors are relevant to our quantitative results. Figure 9 reports the histograms of the errors based on 1 million monthly periods simulated from each algorithm. Panels A and D show that the projection algorithm is (relatively) accurate. The mean job creation equation error, e_t^V, is 2.79×10^{-7}, its mean absolute error is 3.33×10^{-6}, and its maximum absolute error is 1.5%. Also, the 2.5th, 50th, and 97.5th percentiles of e_t^V are -2.32×10^{-6}, -2.26×10^{-10}, and 2.23×10^{-6}. For the investment Euler equation error, e_t^I, its mean is 3.03×10^{-8}, its mean absolute value is 9.23×10^{-7}, and its maximum absolute value is 0.39%. In addition, the 2.5th, 50th, and 97.5th percentiles of e_t^I are 1.14×10^{-6}, 4.69×10^{-11}, and 1.18×10^{-6}. These errors seem mostly acceptable. Ideally, we would like the maximum absolute value of e_t^V to be an order of magnitude smaller than the current level of 1.5% (by further increasing the number of grid points of employment and capital). However, as noted, with the current grid, we need to solve a system of 340,000 nonlinear equations. Even with a reasonable initial guess, the projection algorithm takes a bit more than 6 days to converge on a Dell workstation with 32 3.1-GHz central processing units (CPUs) and 384 GB of physical memory.

From Panels B and E in Figure 9, log linearization is inaccurate. The mean job creation equation error is 1.59%, its mean absolute error is 1.8%, its maximum absolute error is 27.16%, and its 2.5th, 50th, and 97.5th percentiles are −0.5%, 0.63%, and 8.76%, respectively. The mean investment Euler equation error is -4.82×10^{-6}, the mean absolute error is 7.95×10^{-6}, and the maximum absolute error is 1.29×10^{-4}. It is curious that the maximum absolute investment error is even smaller than that from projection. The small error is an illusion, however. The model economy from projection often wanders far from the steady state, but the log-linear economy stays within a small neighborhood surrounding the deterministic steady state.

Figure 10 reports the scatter plots of employment against capital from the model's ergodic distribution based on each algorithm. The deterministic steady state is 0.943 for employment and is 35.29 for capital. Panel A shows that simulations based on the projection solution cover a wide range from 0.225 to 0.963 for employment and from 10 to 40.45 for capital. The lower bounds of the grids rarely bind, with the binding frequency being 0.00039% for employment and 0.01% for capital. In any event, our quantitative results are robust to the grid parameters (Section 3.6). As a testimony for the strong nonlinearity of the PZK model, the maximum employment in simulations, 0.963, is close to the steady state of 0.943, but the minimum employment, 0.225, is substantially far away.

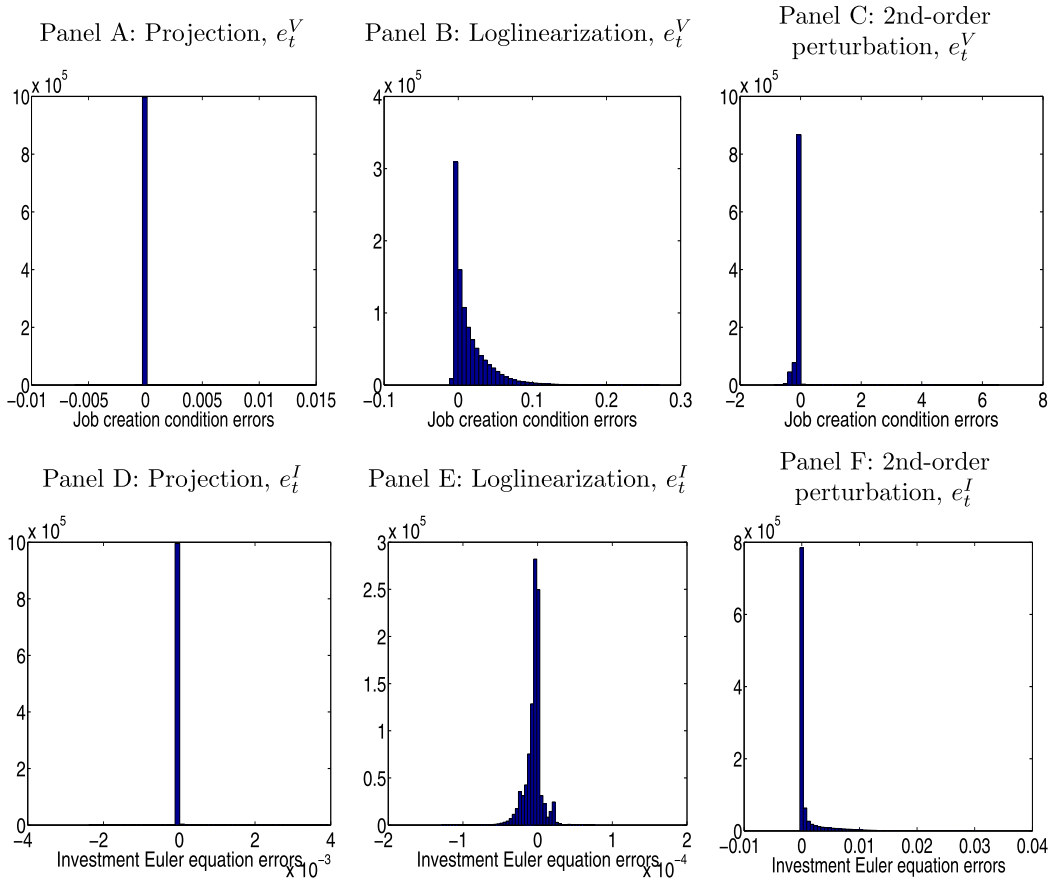

FIGURE 9. Euler equation errors in simulations in the PZK model. We simulate 1 million monthly periods from the model's ergodic distribution based on each algorithm, and plot the histograms for the job creation equation errors, e_t^V, defined in equation (22), and the investment Euler equation errors, e_t^I, defined in equation (23). The underlying log productivity series, x_t, is identical across all the panels.

In contrast, Panel B shows that the log-linear economy covers only a small area from 0.839 to 0.99 for employment and from 28.9 to 41.5 for capital in simulations. Although the minimum employment is further from the steady state than the maximum employment, the extent of the nonlinearity is negligible relative to that from the projection algorithm. Also, the distribution of capital in simulations is largely symmetric, as the distance between the lowest capital and the steady state is close to that between the highest capital and the steady state. The small capital range of the log-linear economy likely explains why its maximum absolute investment Euler equation error is smaller than that from the projection algorithm.

Turning our attention to the second-order perturbation in logs, Panels C and F of Figure 9 show that this algorithm can be dramatically inaccurate, particularly for the job creation equation. For the errors from this equation, e_t^V, the mean is -4.06%, the mean absolute value is 4.51%, and the maximum absolute value is 654.6%. The 2.5th, 50th, and

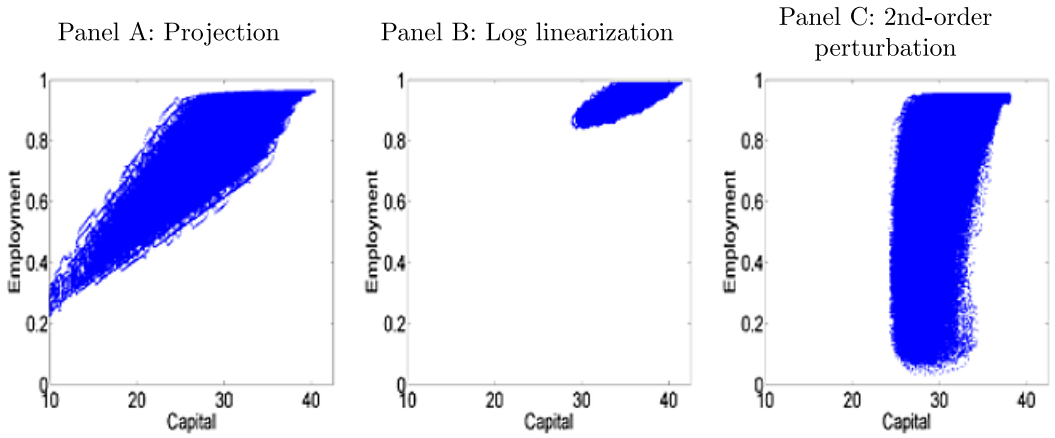

FIGURE 10. The scatter plots of employment versus capital in the PZK model. We simulate 1 million monthly periods from the model's ergodic distribution based on each algorithm, and present the scatter plots of employment against capital.

97.5th percentiles are −32.23%, −0.23%, and 0.26%, respectively. The investment Euler equation errors, e_t^I, are more sensible. The mean is 7.56×10^{-4}, the mean absolute value is 7.72×10^{-4}, and the maximum absolute value is 3.02%. The 2.5th, 50th, and 97.5th percentiles are -6.51×10^{-5}, 2.25×10^{-6}, and 0.82%, respectively. Also, the correlations of the simulated log productivity, x_t, are −0.4 with $|e_t^V|$ and −0.45 with $|e_t^I|$. As such, the algorithm does particularly poorly in bad times.

The employment–capital scatter plot in Panel C of Figure 10 sheds further light on why the second-order perturbation performs particularly poorly in approximating the job creation equation. The simulated economy covers a wide range of employment from 0.03 to 0.954, and the minimum employment is substantially lower than 0.225 from the projection algorithm. Intuitively, the second-order coefficients calculated locally around the deterministic steady state induce very large errors when the economy wanders far away from the steady state.

Because of the large Euler residuals from the second-order perturbation, we do not focus on the moments from this algorithm. Tables 3 and 4 show that the volatilities from the second-order perturbation are substantially higher than those from projection and log linearization. The unemployment–vacancy correlation is even positive, 0.061, as opposed to negative in both log linearization and projection. Because these moments are likely contaminated by large errors, we discard them from further discussion.

3.5 *How does projection deviate from log linearization?*

Table 3 shows that the volatilities from the projection algorithm are higher than those from log linearization. The output, consumption, and investment growth volatilities are 3.26%, 2.60%, and 4.45% per annum with projection, which are higher than 1.72%, 2.41%, and 3.26% with log linearization, respectively. In contrast, the autocorrelations of the three growth rates are largely comparable across the two algorithms.

The labor market moments differ even more between projection and log linearization. The mean unemployment rate is 5.75% with log linearization, which is only about one-half of that with projection, 10.75% (Table 3). In addition, Table 4 shows that log linearization understates the unemployment volatility, but overstates the market tightness volatility and the magnitude of the unemployment–vacancy correlation. Quantitatively, the unemployment volatility is 0.133 with log linearization, which is lower than 0.158 with projection. More drastically, the market tightness volatility is 0.355 with log linearization, which is higher than 0.254 with projection. Finally, the unemployment–vacancy correlation is −0.536 with log linearization, which is higher in magnitude than −0.359 with projection.

To shed light on the intuition behind these results, Figure 11 shows the scatter plots of unemployment, vacancy, and the market tightness against the log productivity in simulations from both projection and log linearization. Similar to the HM model, comparing the plots from projection with those from log linearization clearly shows strong

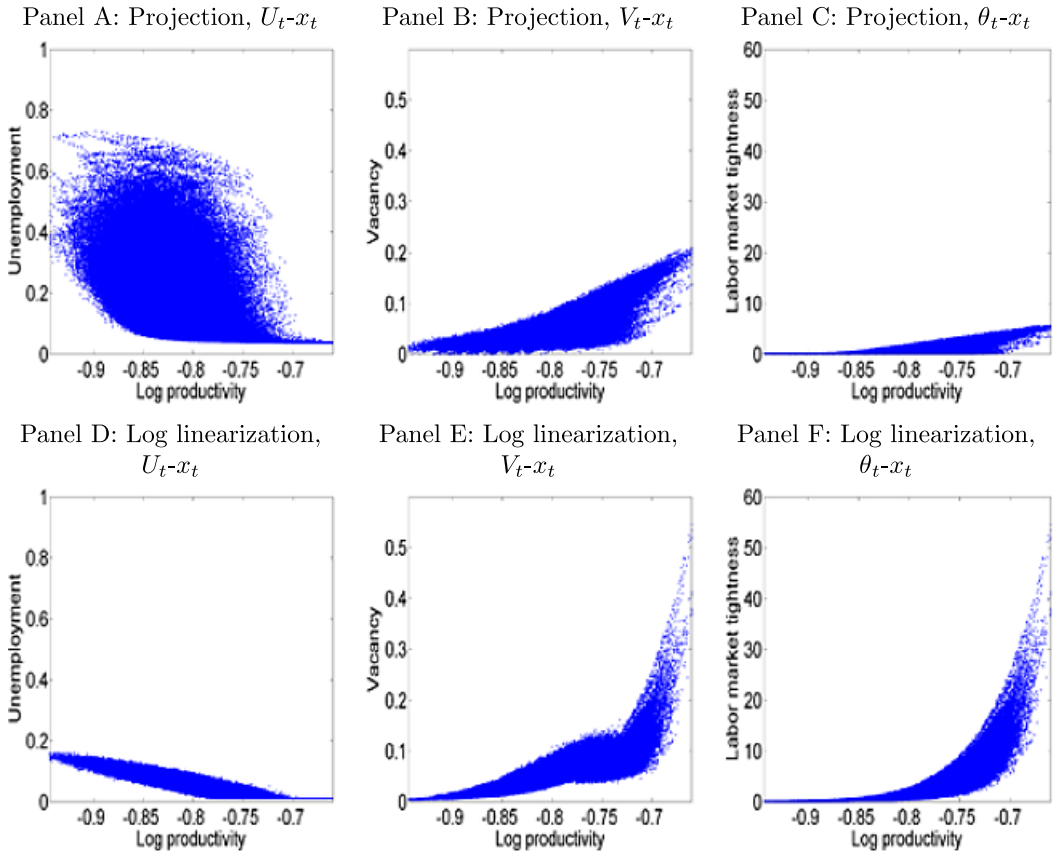

FIGURE 11. Unemployment, vacancy, and labor market tightness in simulations in the PZK model. We simulate 1 million months from the model's ergodic distribution, and present the scatter plots of employment, U_t, vacancy, V_t, and labor market tightness, θ_t, against the log productivity, x_t.

nonlinearity at work. As noted, in recessions, congestion externality and wage inertia combine to cause the unemployment rates to spike up. The projection algorithm fully captures this nonlinear effect (Panel A), but log linearization misses it (almost) entirely (Panel D). In contrast, in booms, vacancies rise and unemployment falls only gradually. The projection algorithm again fully captures this nonlinear effect. In contrast, log linearization understates the congestion externality, giving rise to excessively low unemployment (Panel D), excessively high vacancy rates (Panel E), and excessively high labor market tightness in booms (Panel F).

To further illustrate the differences between projection and log linearization, we report impulse responses. We consider three different initial points: bad, median, and good economies. The bad economy is the 5th percentile of the model's projection-based trivariate distribution of employment, capital, and log productivity, the median economy is the 50th percentile, and the good economy is the 95th percentile. In particular, the unemployment rates are 32.21%, 6.36%, and 4.14%, the capital stocks are 25.13, 34.7, and 37.51, and the log productivity levels are -0.860, -0.802, and -0.744, respectively. We compute the responses to a 1 standard deviation shock to the log productivity, both positive and negative, starting from a given initial point. The impulse responses are averaged across 5000 simulations, each with 60 months.

Figure 12 shows several important nonlinear patterns. First, the projection-based responses in unemployment are substantially stronger in the bad economy than in the good economy. In particular, in response to a negative impulse, the unemployment rate jumps up by 1.35% in the bad economy (Panel A), but only by 0.035% in the good economy (Panel C). The maximum response in the median economy is 0.215%, which is much closer to the good economy than to the bad economy. The large response in the bad economy is largely missed by log linearization, which implies a maximum response of only 0.327%, less than 25% of the projection-based response, 1.35%.

Second, the log linearization-based responses in the market tightness, θ_t, are substantially larger in the good economy than in the bad economy. In particular, in response to a positive impulse, θ_t jumps up by 2.38 in the good economy (Panel F), but only by 0.134 in the bad economy (Panel D). In contrast, the projection algorithm accurately captures the gradual nature of economic expansions. The maximum response in the market tightness is 0.168 in the good economy, which is not far from the response of 0.109 in the bad economy. Finally, wages are again inertial in the projection solution. Relative to projection, log linearization vastly overstates the elasticity of wages in the good economy (Panel I).

Figure 13 shows that the projection-based responses in output, consumption, and investment are all stronger in the bad economy than in the good economy. In particular, in response to a positive impulse, the output, consumption, and investment rise by 2.23%, 1.72%, and 3.34% in the bad economy, in contrast to 0.68%, 0.42%, and 0.89%, respectively, in the good economy. Although close to the projection-based responses in the good economy, log linearization understates the responses in output, consumption, and investment in the bad economy to be 1.17%, 0.76%, and 1.76%, which are only 52.47%, 44.19%, and 52.69% of the projection-based responses, respectively.

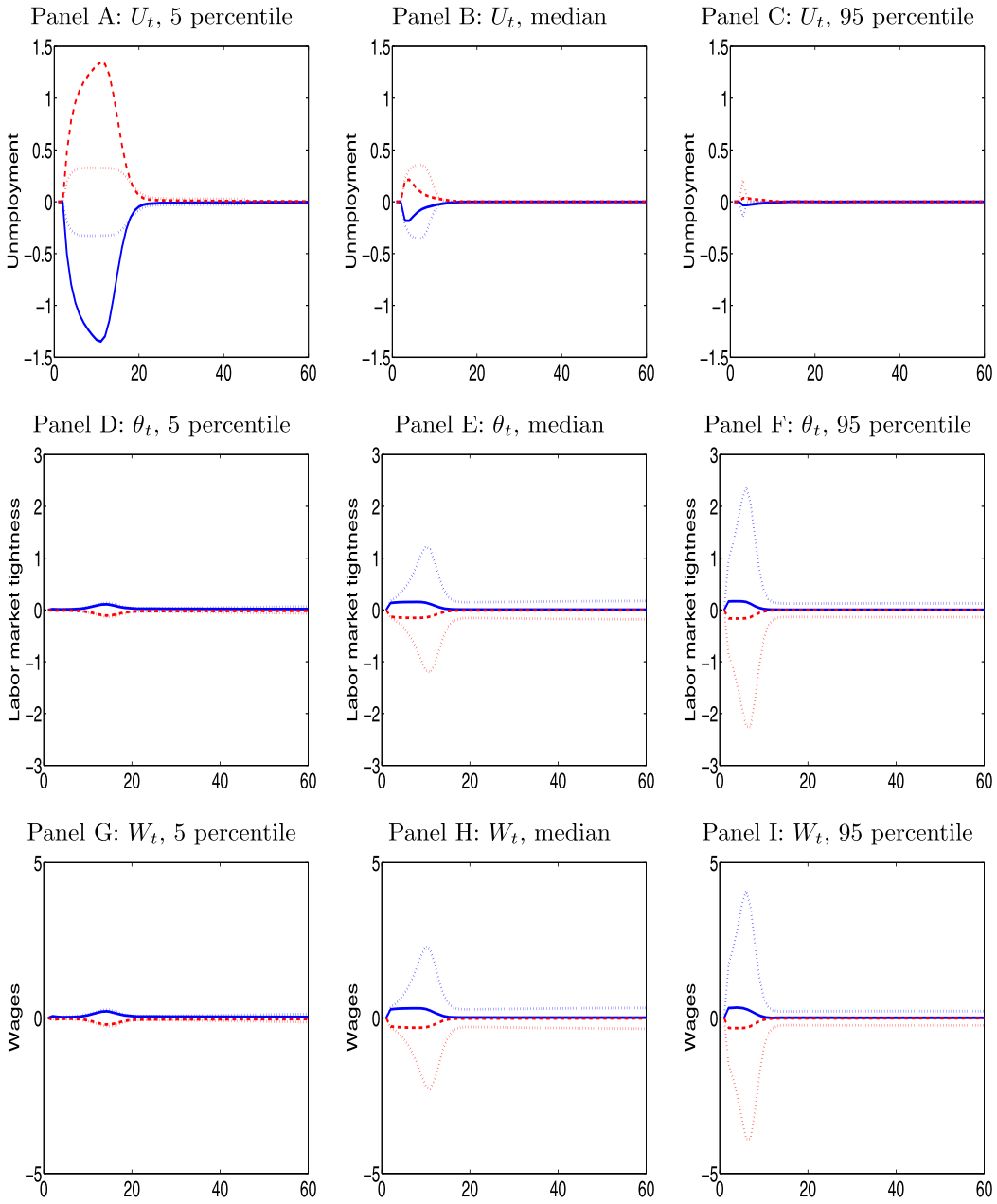

FIGURE 12. Nonlinear impulse responses of unemployment, U_t, labor market tightness, θ_t, and wages, W_t, in the PZK model. The solid (broken) lines are the projection responses to a positive (negative) 1 standard deviation shock to the log productivity. The dotted lines are the corresponding responses from log linearization. The U_t responses are changes in levels (in percent), the θ_t responses are changes in levels, and the W_t responses are changes in levels (in percent) scaled by the respective pre-impulse level.

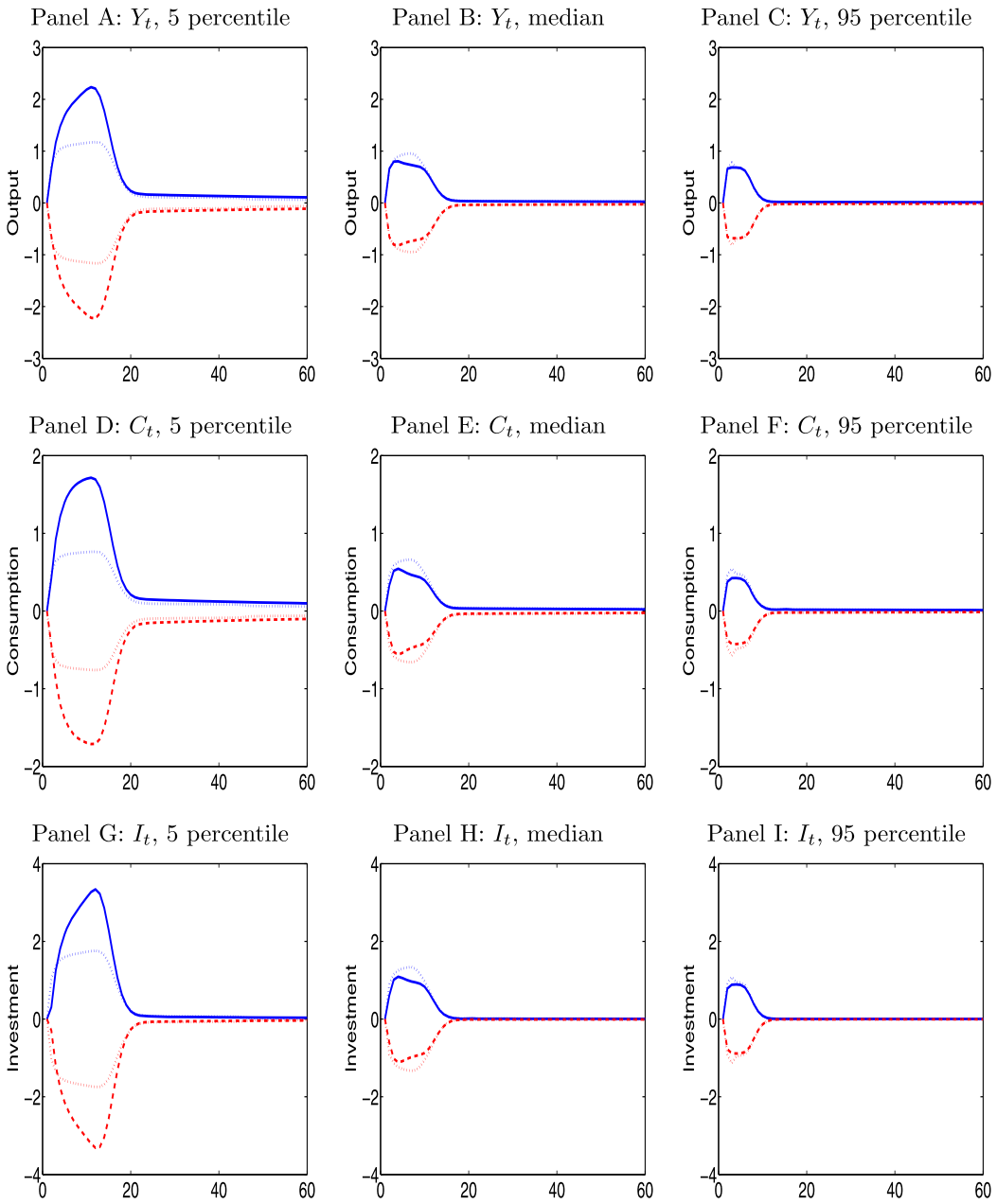

FIGURE 13. Nonlinear impulse responses of output, Y_t, consumption, C_t, and investment, I_t, in the PZK model. The solid (broken) lines are the projection responses to a positive (negative) 1 standard deviation shock to the log productivity. The dotted lines are the corresponding responses from log linearization. All the responses are changes in levels (in percent) scaled by the respective pre-impulse level.

TABLE 5. Robustness of business cycle moments from the projection algorithm for the PZK model.

	σ_Y	ρ_1^Y	ρ_2^Y	ρ_3^Y	ρ_4^Y	σ_C	ρ_1^C	ρ_2^C	ρ_3^C	ρ_4^C
$n_N = n_K = 100$, splines, $\underline{N} = 0.225$, $\underline{K} = 10$	3.26	0.21	−0.08	−0.06	−0.06	2.60	0.23	−0.06	−0.05	−0.05
$n_N = 150$, $n_K = 50$, splines, $\underline{N} = 0.225$, $\underline{K} = 10$	3.25	0.21	−0.08	−0.06	−0.06	2.60	0.23	−0.06	−0.05	−0.05
$n_N = 100$, $n_K = 50$, splines, $\underline{N} = 0.225$, $\underline{K} = 10$	3.25	0.21	−0.07	−0.06	−0.06	2.60	0.23	−0.06	−0.05	−0.05
$n_N = n_K = 50$, splines, $\underline{N} = 0.225$, $\underline{K} = 10$	3.25	0.21	−0.07	−0.06	−0.06	2.60	0.23	−0.06	−0.05	−0.05
$n_N = n_K = 30$, splines, $\underline{N} = 0.25$, $\underline{K} = 10$	3.25	0.21	−0.08	−0.06	−0.06	2.60	0.23	−0.06	−0.05	−0.05
$n_N = n_K = 20$, Chebychev, $\underline{N} = 0.325$, $\underline{K} = 12.5$	3.23	0.21	−0.08	−0.06	−0.06	2.60	0.23	−0.06	−0.05	−0.05

	σ_I	ρ_1^I	ρ_2^I	ρ_3^I	ρ_4^I	$E[U]$	$\overline{\lvert e_t^V \rvert}$	$\overline{\lvert e_t^I \rvert}$
$n_N = n_K = 100$, splines, $\underline{N} = 0.225$, $\underline{K} = 10$	4.45	0.19	−0.10	−0.08	−0.07	10.75	1.50	0.39
$n_N = 150$, $n_K = 50$, splines, $\underline{N} = 0.225$, $\underline{K} = 10$	4.45	0.19	−0.10	−0.08	−0.07	10.70	2.94	0.52
$n_N = 100$, $n_K = 50$, splines, $\underline{N} = 0.225$, $\underline{K} = 10$	4.44	0.19	−0.10	−0.08	−0.07	10.72	2.69	0.57
$n_N = n_K = 50$, splines, $\underline{N} = 0.225$, $\underline{K} = 10$	4.45	0.19	−0.10	−0.08	−0.07	10.71	2.81	0.69
$n_N = n_K = 30$, splines, $\underline{N} = 0.25$, $\underline{K} = 10$	4.45	0.19	−0.10	−0.08	−0.07	10.70	7.08	0.94
$n_N = n_K = 20$, Chebychev, $\underline{N} = 0.325$, $\underline{K} = 12.5$	4.37	0.19	−0.10	−0.08	−0.07	10.31	6.58	0.84

Note: The number of grid points for employment is denoted n_N and that for capital is n_K; $\underline{N}$ is the lower bound for the employment grid (the upper bound is 0.975) and $\underline{K}$ is the lower bound for the capital grid (the upper bound is 42.5); σ_Y, σ_C, and σ_I are the volatilities (in percent), and ρ_j^Y, ρ_j^C, and ρ_j^I are the jth-order autocorrelations of the log output, consumption, and investment growth rates, respectively; $E[U]$ is the mean unemployment rate in percent. We simulate 5000 samples from each variation of the projection algorithm, time–aggregate monthly output, consumption, and investment to annual series, and report cross-simulation averaged results. The maximum job creation equation error, $\overline{\lvert e_t^V \rvert}$, and the maximum investment Euler equation error, $\overline{\lvert e_t^I \rvert}$, both of which are in percent, are calculated from simulations of 1 million monthly periods based on each variation of the algorithm. We experiment with both the finite element method with cubic splines (splines) and the spectral method with Chebychev polynomials (Chebychev).

3.6 *Robustness*

Our results are robust to choices in the grid parameters as well as the basis and degree of function approximation. Tables 5 and 6 report business cycle moments and labor market moments, respectively, from each variation of the projection algorithm. We vary the number of grid points for employment and capital from 20 to 150, and vary the lower bound of the employment grid from 0.225 to 0.325. In each variation, we make sure that the lower bounds for both employment and capital bind no more frequently than 0.02% in simulations. (The more grid points that we use, the more frequently the lower bounds tend to bind in simulations.) We also experiment with the finite element method with cubic splines and the spectral method with Chebychev polynomials.

Table 5 shows that business cycle moments are robust. The consumption growth moments are identical up to two digits after the decimal, and the output growth moments differ only in the second digit after the decimal. The investment growth moments also differ only in the second digit, except for the Chebychev approximation, which gives rise to an investment growth volatility of 4.37%, in contrast to 4.45% in our benchmark implementation with cubic splines. The Chebychev approximation also implies a mean unemployment rate of 10.31%, whereas the mean unemployment rates from splines vary from 10.7% to 10.75%. In addition, Table 6 shows quantitatively similar results for

TABLE 6. Robustness of labor market moments from the projection algorithm for the PZK model.

	U	V	θ	Y/N		U	V	θ	Y/N
	$n_N = n_K = 100$, Splines, $\underline{N} = 0.225$, $\underline{K} = 10$					$n_N = 150$, $n_K = 50$, Splines, $\underline{N} = 0.225$, $\underline{K} = 10$			
Standard deviation	0.158	0.158	0.254	0.010		0.158	0.158	0.254	0.010
Autocorrelation	0.844	0.588	0.763	0.657		0.844	0.589	0.764	0.658
Correlation matrix		−0.359	−0.473	−0.337	U		−0.359	−0.473	−0.338
			0.899	0.983	V			0.899	0.983
				0.930	θ				0.930
	$n_N = 100$, $n_K = 50$, Splines, $\underline{N} = 0.225$, $\underline{K} = 10$					$n_N = n_K = 50$, Splines, $\underline{N} = 0.225$, $\underline{K} = 10$			
Standard deviation	0.158	0.158	0.254	0.010		0.159	0.158	0.254	0.010
Autocorrelation	0.844	0.589	0.764	0.658		0.844	0.589	0.764	0.658
Correlation matrix		−0.359	−0.473	−0.338	U		−0.358	−0.472	−0.338
			0.899	0.983	V			0.899	0.983
				0.930	θ				0.930
	$n_N = n_K = 30$, Splines, $\underline{N} = 0.25$, $\underline{K} = 10$					$n_N = n_K = 20$, Chebychev, $\underline{N} = 0.325$, $\underline{K} = 12.5$			
Standard deviation	0.159	0.158	0.254	0.010		0.160	0.157	0.254	0.010
Autocorrelation	0.844	0.589	0.764	0.659		0.845	0.593	0.767	0.665
Correlation matrix		−0.358	−0.472	−0.337	U		−0.361	−0.474	−0.341
			0.898	0.982	V			0.899	0.981
				0.929	θ				0.929

Note: The number of grid points for employment is denoted n_N and that for capital is n_K; $\underline{N}$ is the lower bound for the employment grid (the upper bound is 0.975) and $\underline{K}$ is the lower bound for the capital grid (the upper bound is 42.5). We simulate 5000 artificial samples with 768 months in each sample from each variation of the projection algorithm. We take the quarterly averages of monthly unemployment, U, vacancy, V, and labor productivity, Y/N, to convert to 256 quarters. Labor market tightness is denoted $\theta = V/U$. All the variables are in HP-filtered proportional deviations from the mean with a smoothing parameter of 1600. All the model moments are cross-simulation averages. We experiment with both the finite element method with cubic splines (splines) and the spectral method with Chebychev polynomials (Chebychev).

labor market moments. These moments mostly differ only in the third digit after the decimal across alternative variations of the algorithm.

The alternative variations of the projection algorithm differ only in the maximum absolute Euler equation errors. From Table 5, the benchmark implementation with 100 grid points for both employment and capital gives rise to a maximum absolute job creation equation error of 1.5% and a maximum absolute investment Euler equation error of 0.39% in simulations of 1 million monthly periods. In contrast, the three versions with 50 grid points for capital imply maximum absolute job creation errors that vary from 2.69% to 2.94% and maximum investment Euler equation errors that vary from 0.52% to 0.69%. The smaller grid with 30 points for both employment and capital are sufficient to obtain accurate model moments quantitatively. However, this implementation yields a maximum absolute job creation error of 7.08%.

4. Conclusion

An accurate global algorithm is critical for quantifying the basic moments of the Diamond–Mortensen–Pissarides model. Log linearization understates the mean and volatility of unemployment, but overstates the volatility of labor market tightness as well as the magnitude of the unemployment–vacancy correlation. Also, log linearization understates the impulse responses in unemployment in recessions, but overstates the responses in the market tightness in booms. Finally, as the economy wanders far away from the deterministic steady state, the second-order perturbation in logs induces severe Euler equation errors, which are often much larger than those from log linearization. Our work highlights the extreme importance of accurately accounting for nonlinear dynamics in quantitative macroeconomic studies.

Two remarks are in order. First, we use the Hagedorn–Manovskii (2008) small-surplus calibration as an illustration because of their prominence in the macro labor literature. However, any DMP models with realistic unemployment volatilities are likely to contain strong nonlinear dynamics. In particular, Ljungqvist and Sargent (2016) show that all the proposed DMP models in the literature induce strong responses of unemployment to productivity shocks by diminishing the fundamental surplus, which is defined as the amount of output allocated to vacancy creation. The list of models includes Hagedorn and Manovskii as well as the Hall (2005) sticky-wage model, the Hall–Milgrom (2008) alternating bargaining model, and the Pissarides (2009) fixed matching costs model. As such, our insight on accurately accounting for nonlinearities is general, not specific to Hagedorn and Manovskii. Second, we focus on log linearization and second-order perturbation because these methods are used extensively in the empirical macroeconomics literature Christiano, Eichenbaum, and Evans (2005), Smets and Wouters (2007). We emphasize that our work is silent about the performance of high-order perturbations. Evaluating the performance of state-of-the-art high-order perturbation methods against our accurate global algorithm in the context of the DMP model seems to be an important direction for future research.

Appendix: Dynare programs

A.1 *The HM model*

```
// HM_loglinear.mod


var N, x, C;
predetermined_variables N;
varexo e;


parameters bet, rhox, stdx, eta, b, s, iota, kappa_K, kappa_W, xi;
bet     = 0.99^(1/12);
rhox    = 0.9895;
stdx    = 0.0034;
eta     = 0.052;
b       = 0.955;
```

```
s       = 0.0081;
iota    = 0.407;
kappa_K = 0.474;
kappa_W = 0.11;
xi      = 0.449;


model;
# kappa_t = kappa_K*exp(x) + kappa_W*(exp(x)^xi);
# V       = (exp(x)*exp(N) - exp(C))/kappa_t;
# theta   = V/(1 - exp(N));
# q       = (1 + theta^iota)^(-1/iota);
# kappa_p = kappa_K*exp(x(+1)) + kappa_W*(exp(x(+1))^xi);
# V_p     = ( exp(x(+1))*exp(N(+1)) - exp(C(+1)) )/kappa_p;
# theta_p = V_p/(1 - exp(N(+1)));
# q_p     = (1 + theta_p^iota)^(-1/iota);
# W_p     = eta*(exp(x(+1)) + kappa_p*theta_p) + (1 - eta)*b;


exp(N(+1)) = (1 - s)*exp(N) + q*V;
kappa_t/q  = bet*( exp(x(+1)) - W_p + (1 - s)*kappa_p/q_p );
x          = rhox*x(-1) + e;
end;


initval;
N = log(1 - 0.1);
x = 0;
e = 0;
end;


steady;
check;


shocks;
var e = stdx^2;
end;


stoch_simul (order = 1, nocorr, nomoments, IRF = 0);
```

For the second-order perturbation solution in logs, we change the last command to

```
stoch_simul (order = 2, nocorr, nomoments, IRF = 0);
```

A.2 *The PZK model*

```
// PZK_loglinear.mod


var  N, K, x, C, I, theta;
predetermined_variables  N, K;
varexo e;
```

```
parameters  beta, xbar, rhox, stdx, alpha, delta, nu, eta, s, iota, b, kappa;
beta    =  0.99^(1/3);
xbar    = -0.802;
rhox    =  0.983047572491559;
stdx    =  0.0065;
alpha   =  1/3;
delta   =  0.01;
nu      =  2;
eta     =  0.04;
s       =  0.035;
iota    =  1.25;
b       =  0.95;
kappa   =  0.45;


model;
# a1    = delta/(1 - nu);
# a2    = delta^(1/nu);
# Phi   = (a1 + (a2/(1-1/nu))*((exp(I)/exp(K))^(1-1/nu)))*exp(K);
# q     = (1 + exp(theta)^iota)^(-1/iota);
# qp    = (1 + exp(theta(+1))^iota)^(-1/iota);
# Y     = exp(x)*(exp(K)^alpha)*(exp(N)^(1 - alpha));
# V     = (Y - exp(C) - exp(I))/kappa;
# M     = beta*( exp(C)/exp(C(+1)) );
# Yp    = exp(x(+1))*(exp(K(+1))^alpha)*(exp(N(+1))^(1 - alpha));
# Wp    = eta*((1 - alpha)*Yp/exp(N(+1)) + kappa*exp(theta(+1))) + (1 - eta)*b;


exp(theta) = V/(1 - exp(N));
exp(N(+1)) = (1 - s)*exp(N) + q*V;
kappa/q   = M*( (1 - alpha)*Yp/exp(N(+1)) - Wp + (1 - s)*kappa/qp );
exp(K(+1)) = (1 - delta)*exp(K) + Phi;
(1/a2)*((exp(I)/exp(K))^(1/nu)) = M*(alpha*Yp/exp(K(+1))
  + (1/a2)*((exp(I(+1))/exp(K(+1)))^(1/nu))*(1 - delta + a1)
 + (1/(nu-1))*exp(I(+1))/exp(K(+1)));
x          = xbar*(1 - rhox) + rhox*x(-1) + e;
end;


initval;
N     = log(1 - 0.048828933192708);
K     = log(35.613860128463763);
x     = xbar;
C     = log(0.997225855318108);
I     = log(0.356138601284638);
theta = log(2.234716290234390);
e     = 0;
end;


steady;
check;


shocks;
```

```
var e = stdx^2;
end;


stoch_simul (order = 1, nocorr, nomoments, IRF = 0);
```

For the second-order perturbation solution in logs, we change the last command to
`stoch_simul (order = 2, nocorr, nomoments, IRF = 0);`

References

Adjemian, S., H. Bastani, M. Juillard, F. Mihoubi, G. Perendia, M. Ratto, and S. Villemot (2011), "Dynare: Reference manual, version 4." Dynare working paper 1, CEPREMAP. [617]

Algan, Y., O. Allais, and W. J. Den Haan (2010), "Solving the incomplete markets model with aggregate uncertainty using parameterized cross-sectional distributions." *Journal of Economic Dynamic and Control*, 34, 59–68. [613]

Andolfatto, D. (1996), "Business cycles and labor-market search." *American Economic Review*, 86, 112–132. [611]

Aruoba, S. B., J. Fernández-Villaverde, and J. F. Rubio-Ramírez (2006), "Comparing solution methods for dynamic equilibrium economies." *Journal of Economic Dynamic and Control*, 30, 2477–2508. [613]

Barnichon, R. (2010), "Building a composite help-wanted index." *Economic Letters*, 109, 175–178. [633]

Blanchard, O. and J. Gali (2010), "Labor markets and monetary policy: A new Keynesian model with unemployment." *American Economic Journal: Macroeconomics*, 2, 1–30. [612]

Caldara, D., J. Fernández-Villaverde, J. F. Rubio-Ramírez, and W. Yao (2012), "Computing DSGE models with recursive preferences and stochastic volatility." *Review of Economic Dynamics*, 15, 188–206. [613]

Christiano, L. J., M. Eichenbaum, and C. L. Evans (2005), "Nominal rigidities and the dynamic effects of a shock to monetary policy." *Journal of Political Economy*, 113, 1–45. [644]

Christiano, L. J. and J. D. M. Fisher (2000), "Algorithms for solving dynamic models with occasionally binding constraints." *Journal of Economic Dynamics and Control*, 24, 1179–1232. [613, 616]

Den Haan, W. J. (2010), "Comparison of solutions to the incomplete markets model with aggregate uncertainty." *Journal of Economic Dynamics and Control*, 34, 4–27.

Den Haan, W. J. (2011), "Dynare." Lecture notes, London School of Economics. [617]

Den Haan, W. J., G. Ramey, and J. Watson (2000), "Job destruction and propagation of shocks." *American Economic Review*, 90, 482–498. [614, 633]

Den Haan, W. J. and P. Rendahl (2010), "Solving the incomplete markets model with aggregate uncertainty using explicit aggregation." *Journal of Economic Dynamics and Control*, 34, 69–78. [613]

Diamond, P. A. (1982), "Wage determination and efficiency in search equilibrium." *Review of Economic Studies*, 49, 217–227. [611]

Fernández-Villaverde, J. and O. Levintal (2016), "Solution methods for models with rare disasters." NBER working paper. [613]

Fernández-Villaverde, J., J. F. Rubio-Ramírez, and F. Schorfheide (2016), "Solution and estimation methods for DSGE models." In *Handbook of Macroeconomics*, Vol. 2 (J. Taylor and H. Uhlig, eds.), 527–724, North-Holland. [631]

Gertler, M. and A. Trigari (2009), "Unemployment fluctuations with staggered Nash wage bargaining." *Journal of Political Economy*, 117, 38–86. [611, 612, 633]

Hagedorn, M. and I. Manovskii (2008), "The cyclical behavior of equilibrium unemployment and vacancies revisited." *American Economic Review*, 98, 1692–1706. [611, 612, 613, 614, 630, 644]

Hall, R. E. (2005), "Employment fluctuations with equilibrium wage stickiness." *American Economic Review*, 95, 50–65. [611, 644]

Hall, R. E. and P. R. Milgrom (2008), "The limited influence of unemployment on the wage bargain." *American Economic Review*, 98, 1653–1674. [612, 644]

Hodrick, R. J. and E. C. Prescott (1997), "Postwar U.S. business cycles: An empirical investigation." *Journal of Money, Credit, and Banking*, 29, 1–16. [617]

Jermann, U. J. (1998), "Asset pricing in production economies." *Journal of Monetary Economics*, 41, 257–275. [630]

Judd, K. L. (1992), "Projection methods for solving aggregate growth models." *Journal of Economic Theory*, 58, 410–452. [613, 624, 634]

Judd, K. L. (1998), *Numerical Methods in Economics*. The MIT Press, Cambridge, Massachusetts. [616]

Judd, K. L., L. Maliar, S. Maliar, and R. Valero (2014), "Smolyak method for solving dynamic economic models: Lagrange interpolation, anisotropic grid, and adaptive domain." *Journal of Economic Dynamics and Control*, 44, 92–123. [631]

Kollmann, R., S. Maliar, B. A. Malin, and P. Pichler (2011), "Comparison of solutions to the multi-country real business cycle model." *Journal of Economic Dynamics and Control*, 35, 186–202. [613]

Kopecky, K. A. and R. M. H. Suen (2010), "Finite state Markov-chain approximations to highly persistent processes." *Review of Economic Dynamics*, 13, 701–714. [628]

Ljungqvist, L. and T. J. Sargent (2016), "The fundamental surplus." Working paper, New York University. [644]

Maliar, L., S. Maliar, and F. Valli (2011), "Solving the incomplete markets model with aggregate uncertainty using the Krusell–Smith algorithm." *Journal of Economic Dynamics and Control*, 34, 42–49. [613]

Maliar, S., L. Maliar, and K. L. Judd (2011), "Solving the multi-country real business cycle model using ergodic set methods." *Journal of Economic Dynamics and Control*, 35, 207–228. [613]

Malin, B. A., D. Krueger, and F. Kubler (2011), "Solving the multi-country real business cycle model using a Smolyak-collocation method." *Journal of Economic Dynamics and Control*, 35, 229–239. [613]

Merz, M. (1995), "Search in labor market and the real business cycle." *Journal of Monetary Economics*, 95, 269–300. [611, 614]

Miranda, M. J. and P. L. Fackler (2002), *Applied Computational Economics and Finance*. The MIT Press, Cambridge, Massachusetts. [616]

Mortensen, D. T. (1982), "The matching process as a noncooperative bargaining game." In *The Economics of Information and Uncertainty* (J. J. McCall, ed.), 233–254, University of Chicago Press, Chicago. [611]

Mortensen, D. T. and É. Nagypál (2007), "More on unemployment and vacancy fluctuations." *Review of Economic Dynamics*, 10, 327–347. [611]

Petrosky-Nadeau, N. and E. Wasmer (2013), "The cyclical volatility of labor markets under frictional financial market." *American Economic Journal: Macroeconomics*, 5, 193–221. [612]

Petrosky-Nadeau, N. and L. Zhang (2013), "Unemployment crises." Working paper, Federal Reserve Bank of San Francisco and The Ohio State University. [633]

Petrosky-Nadeau, N., L. Zhang, and L. Kuehn (2015), "Endogenous disasters." Working paper, Federal Reserve Bank of San Francisco and The Ohio State University. [612, 613, 614, 619]

Pichler, P. (2011), "Solving the multi-country real business cycle model using a monomial rule Galerkin method." *Journal of Economic Dynamics and Control*, 35, 240–251. [613]

Pissarides, C. A. (1985), "Short-run dynamics of unemployment, vacancies, and real wages." *American Economic Review*, 75, 676–690. [611]

Pissarides, C. A. (2009), "The unemployment volatility puzzle: Is wage stickiness the answer?" *Econometrica*, 77, 1339–1369. [611, 644]

Rouwenhorst, K. G. (1995), "Asset pricing implications of equilibrium business cycle models." In *Frontiers of Business Cycle Research* (T. Cooley, ed.), 294–330, Princeton University Press, Princeton. [613, 616, 625]

Shimer, R. (2005), "The cyclical behavior of equilibrium unemployment and vacancies." *American Economic Review*, 95, 25–49. [611]

Smets, F. and R. Wouters (2007), "Shocks and frictions in US business cycles: A Bayesian DSGE approach." *American Economic Review*, 97, 586–606. [644]

Tauchen, G. (1986), "Finite state Markov-chain approximations to univariate and vector autoregressions." *Economics Letters*, 20, 177–181. [613, 616, 626, 628]

Co-editor Karl Schmedders handled this manuscript.

Manuscript received 5 May, 2014; final version accepted 4 November, 2016; available online 4 November, 2016.